Heat Stress Interferes with Formation of Double-Strand Breaks and Homology Synapsis in *Arabidopsis thaliana*

Yingjie Ning[1#], Qingpei Liu[2#], Chong Wang[3#], Erdai Qin[1], Zhihua Wu[1], Minghui Wang[4], Ke Yang[1], Ibrahim Eid Elesawi[5, 6, 7], Chunli Chen[5, 6], Hong Liu[1], Rui Qin[1], Bing Liu[1*]

[1]College of Life Sciences, South-Central University for Nationalities, Wuhan 430074, China;
[2]School of Pharmaceutical Sciences, South-Central University for Nationalities, Wuhan 430074, China;
[3]College of Life Sciences, Shanghai Normal University, Shanghai 200234, China;
[4]School of Integrative Plant Science, Cornell University, Ithaca, NY 14853, United States of America;
[5]College of Life Science and Technology, Huazhong Agricultural University, Wuhan, 430070;
[6]Key Laboratory of Horticultural Plant Biology, Huazhong Agricultural University, Wuhan, 430070, China;
[7]Agricultural Biochemistry Department, Faculty of Agriculture, Zagazig University, 44511 Zagazig, Egypt;
[#]Authors with equal contribution;
[*]To whom correspondence should be addressed: Bing Liu (bl472@scuec.edu.cn).

Author contributions

Y.J.N., Q.P.L. and C.W. performed experiment and contributed to data analysis; E.D.Q., Z.H.W. and M.H.W. contributed to transcriptome analysis; K.Y. helped with immunolocalization assays; E.E.I. helped with FISH experiment; C.L.C., H.L. and R.Q. contributed to data analysis; B.L. designed and conceived the project, performed experiment, analyzed data, wrote and edited the manuscript. All the authors have read and approved the manuscript prior to submission.

Abstract

Meiotic recombination (MR) drives reciprocal exchange of genetic information which allows novel combination of alleles and contributes to genomic diversity of eukaryotes. In this study, we report that heat stress (36-38°C) over fertile threshold fully abolishes crossover occurrence by lowering the formation of SPO11-dependent double-strand breaks (DSBs) in Arabidopsis. The high temperature partially suppresses chromosome fragmentation in the *rad51* and *syn1* mutants by reducing DSB formation. In addition, we found that although the SYN1-mediated formation of chromosome axis is not influenced by the high temperature, ASY1-associated axial element of synaptonemal complex (SC) is partially compromised, and the

ZYP1-dependent central element of axis is severely disrupted, indicating that homology synapsis is another prominent target of high temperature. Besides, we observed that the loading of recombinase DMC1 on chromatin is significantly reduced by high temperatures, suggesting that heat stress interferes with DMC1-dependent MR. Moreover, we found that the numbers of DSB and DMC1 keep stable within a limited range of temperature increase, while decrease when the DSB-processing system reaches threshold to heat. Furthermore, transcriptome study revealed a universal variation of the expression of meiotic genes under low (4°C) and high (32°C) temperatures, suggesting that temperature may influence MR by modulating the transcription of MR-related factors. We also found that the landscape of 5-methylcytosine (5mC) was altered under high temperatures, suggesting that environmental temperature may influence the distribution of MR via reshaped DNA methylation status of chromatin. Taken together, our findings provide evidence shedding light on how environment temperatures influence MR in Arabidopsis.

Introduction

Male meiosis is the basis for sexual reproduction and is essentially important for genomic diversity and ploidy stability of plants over generations. Homologous recombination occurs at early stage of meiosis which allows reciprocal exchange of genetic information and assures balanced chromosome segregation at later meiotic stages (Wang and Copenhaver, 2018). Meiotic recombination (MR) is initiated by programmed formation of double-strand breaks (DSBs) which is catalyzed by SPO11, a conserved type II topoisomerase (topoisomerase VI, subunit A) among eukaryotes (Bergerat et al., 1997; Grelon et al., 2001). In Arabidopsis, there are three SPO11 homologues which share 20%-30% sequence identity (Hartung and Puchta, 2000, 2001). SPO11-1 and SPO11-2 are required for MR, while SPO11-3 plays a role in DNA endo-reduplication (Hartung et al., 2007; Stacey et al., 2006; Sugimoto-Shirasu et al., 2002). DSB formation is required for homologous chromosome synapsis and bivalent formation, and both the *spo11-1* and *spo11-2* mutants have defective homology synapsis with resultant formation of univalents at diakinesis and metaphase I, and severely impaired male fertility due to disrupted chromosome segregation (Grelon et al., 2001; Stacey et al., 2006). Contemporaneously, as the initiation of MR, meiosis-specific chromosome axis starts to be formed that aids DSB formation and homologous recombination. HORMA domain protein ASY1 and two coiled-coil proteins ASY3 and ASY4 are essentially required in building of axis (Armstrong et al., 2002; Chambon et al., 2018; Ferdous et al., 2012; Sanchez-Moran et al., 2008). Sister chromatids are bound by meiosis-specific α-kleisin Rec8 and form a loop structure, the basal regions of which are connected to axis (Zickler and Kleckner, 1999). The formation of DSB is proposed to take place at the chromatin loops tethered to the axis, and it was evidenced that loss of function of AtRec8/SYN1 causes reduced DSB formation (Lambing et al., 2020b; Zickler and Kleckner, 1999). DSBs are not evenly distributed along the chromosomes but instead have a defined landscape by chromatin status including histone and DNA epigenetic modifications (Choi et al., 2018; He et al., 2017). Generally, DSB hotspots occur at lower DNA methylation regions (Choi et al., 2018; He et al., 2017; Lambing et al., 2020b). MRE11-RAD50-NBS1/XRS2 (MRN/X) complex generates 3' single-strand

DNAs (ssDNAs) at DSB sites, and two recombinases RAD51 and DMC1 bind to ssDNA overhangs to promote homologous searching and pairing (Hartung et al., 2007; Milman et al., 2009; Neale et al., 2005; Uanschou et al., 2007). DMC1 and RAD51 do not co-localize at DSB sites and function separately (Kurzbauer et al., 2012). RAD51 acts as an accessory factor for the assembly and function DMC1 in catalyzing MR (Cloud et al., 2012; Da Ines et al., 2013; Lan et al., 2020). It has been proposed that RAD51 plays a role in non-crossover (NCO) pathway in DSB repair using sister chromatid as template, while DMC1 is responsible for meiotic-specific DSB repair (Cloud et al., 2012; Singh et al., 2017). Axis element ASY1 is required for the bias of DSB repair towards DMC1-mediated MR (Sanchez-Moran et al., 2007). DSBs are repaired into either COs or NCOs, and most of COs (~85%) are catalyzed through ZMMs pathways; namely type-I COs (interfering-sensitive COs), while the other 15% type-II COs (interfering-insensitive COs) are mediated by MUS81-dependent pathway, reviewed by (Lambing et al., 2017; Wang and Copenhaver, 2018).

Variations of temperature can affect one or more aspects during meiotic cell division including MR and chromosome dynamics (Liu et al., 2019; Morgan et al., 2017). In Arabidopsis, Populus and Persimmon, heat stress affects the formation and organization of spindle and/or phragmoplast during male meiosis, which subsequently causes aberrant chromosome segregation and cytokinesis leading to meiotic restitution and unreduced gametes (Mai et al., 2019; Wang et al., 2017). In the context of MR, increase of temperature within the fertile threshold (28°C) promotes MR rate in Arabidopsis via enhanced type-I CO formation but not by influencing the generation of DSBs (Francis et al., 2007; Lloyd et al., 2018; Modliszewski et al., 2018). A higher temperature at 32°C was recently found to influence homology synapsis and induce non-homology interaction in Arabidopsis (De Storme and Geelen, 2020). At the same time, extreme high temperatures beyond fertile threshold (36-38°C) cause defective chromosome segregation and cytokinesis during male meiosis (Lei et al., 2020). The extreme high temperature severely affects the construction of spindle and phragmoplast leading to production of unreduced microspores and polyads (Lei et al., 2020). These findings indicate that environmental temperature conditions can affect the ploidy stability and genomic diversity of plants by interfering with meiosis. However, the involved mechanism remains unclear. In this study, we demonstrate that increases of temperature interfere with MR by compromising SPO11-depednent DSB formation and SC-dependent homology synapsis. In addition, we found that heat stress also affects DMC1-mediated MR. We showed that the expression of MR-related genes is universally influenced by either the increase or decrease of temperature, suggesting that temperatures influence meiosis via modulated gene expression. Moreover, we observed an altered landscape of DNA methylation on chromatin under high temperatures. Taken together, our findings provide insights into the mechanism underlining how environmental temperatures manipulate MR in *Arabidopsis thaliana*.

Results

High temperatures beyond fertility-tolerable range inhibit bivalent formation

We analyzed the chromosome dynamics during male meiosis I in heat-stressed (36-38°C) flowering wild-type Col-0 plants using 4′,6-diamidino-2-phenylindole (DAPI) staining. Under normal temperature conditions, leptotene chromosomes display long thin threads configurations, and homologous chromosomes start to pair at zygotene thereafter fully synapse at pachytene (Supplement Fig. S1A-C). COs are formed between the synapsed homologous chromosomes which are condensed at diplotene (Supplement Fig. S1D). Five pairs of bivalents are formed at diakinesis representing completion of prophase I (Supplement Fig. S1E). At metaphase I, the five pairs of bivalents condense further and are aligned at cell plate by the bipolar pulling of spindles (Supplement Fig. S1F). Homologous chromosomes are separated at anaphase I, and are temporally decondensed at interkinesis (Supplement Fig. S1G and H). In heat-stressed Col-0 plants, however, although we can find thin threads leptotene and zygotene chromosomes (Supplement Fig. S1I and J), we can hardly find pachytene and/or diplotene chromosomes with accomplished homology synapsis (Supplement Fig. S1K and L). At diakinesis and metaphase I, ten univalents were consistently found indicating that CO formation was abolished (Supplement Fig. S1M-Q). Abnormal connections between the univalents suggesting that the heat stress induces non-homology interaction (Supplement Fig. S1N-P, see red arrows). The omitted bivalent formation caused unbalanced chromosome segregation at anaphase I and interkinesis, consequently leading to the generation of aneuploid spores (Supplement Fig. S1R-T; Supplement Fig. S2A-D). Fluorescence in situ hybridization (FISH) using a centromere-specific probe confirmed that the heat stress abolished bivalent formation (Supplement Fig. S3). These data demonstrate that high temperatures over fertile threshold suppresses CO formation in Arabidopsis.

Heat stress reduces formation of SPO11-dependent DSBs

The univalent formation induced by the heat stress phenocopied plants defective for DSB formation (Supplement Fig. S1M-Q) (De Muyt et al., 2007; Grelon et al., 2001; Huang et al., 2019; Stacey et al., 2006), which drove us to hypothesize that the extreme high temperature abolishes COs by interfering with DSB formation. We therefore examined DSB number in the heat-stressed wild-type Wassilewskija (Ws) and *spo11-1-1* plants by detecting γH2A.X using an anti-γH2A.X antibody, which detects phosphorylated H2A.X histone variants that specifically occur at DSB sites (Kurzbauer et al., 2012). Under normal temperature conditions, wild-type plants showed ~110 γH2A.X foci while the *spo11-1-1* mutant displayed a much lower count (~41) (Fig. 1A-C), indicating for a compromised DSB formation in the *spo11-1-1* plants. After heat stress, we found that the number of γH2A.X foci in the wild-type plants was significantly lowered (~34) (Fig. 1A and D), which, however, was not further reduced in the *spo11-1-1* plants (~33) (Fig. 1A and E). This finding indicated that the high temperature stress reduces SPO11-dependent DSB formation in Arabidopsis.

Heat stress suppresses chromosome fragmentation in *rad51* and *syn1* plants by lowering DSB formation

To validate that heat stress reduces DSB formation, we analyzed the chromosome spread of the *syn1* and *rad51* mutants under heat stress. Loss of function of SYN1 causes chromosome fragmentation in Arabidopsis (Bai et al., 1999). The *syn1* mutant has a low but retained level of DSBs, and both recombinases RAD51 and DMC1 are largely reduced in *syn1* plants, suggesting that chromosome fragmentation in *syn1* result from the compromised DSB repair (Lambing et al., 2020b). We found that chromosomes in *syn1* plants incubated under normal temperature conditions displayed less condensed at diakinesis and are numerously fragmented at metaphase I (Fig. 2A and B). After heat stress, the *syn1* mutant was able to produce ten compacted univalents at both diakinesis and metaphase I stages (Fig. 2C-F), or have less fragmented chromosomes (Fig. 2G), indicating that the chromosome fragmentation in *syn1* plants was partially suppressed by the heat stress. Moreover, aberrant connections between the univalents occurred in the heat-stressed *syn1* plants suggesting that non-homology interaction took place (Fig. 2D and E, see red arrows). The *rad51* mutant has a chromosome fragmentation phenotype due to impaired DSB repair (Su et al., 2017). The double *spo11 rad51* mutant rescues the chromosome fragmentation in *rad51* and displays the phenotype of the singe *spo11* mutant (Hartung et al., 2007). Under control temperature we did not observe typical diakinesis chromosome configuration in the *rad51* mutant (Fig. 2H). In contrast, we were able to find diakinesis-staged pollen mother cells (PMCs) with ten univalents (Fig. 2I), which indicates for an inhibited chromosome fragmentation in *rad51* plants. The chromosome configuration in the heat-stressed *syn1* and *rad51* mutants phenocopied the *spo11-1-1* mutant (Fig. 2J-L) (Su et al., 2017), which thus supported that the heat stress reduces SPO11-dependent DSB formation.

We next examined the γH2A.X number in the heat-treated *syn1* and *rad51* mutants. Under normal temperature conditions, the *syn1* mutant showed significantly less γH2A.X number (~52) than the wild-type plants (~112) (Fig. 2M, N and P), indicating that DSB formation in the *syn1* mutant is strongly interfered, which was in line with the report by (Lambing et al., 2020b). After heat stress, the *syn1* mutant exhibited significantly reduced γH2A.X foci (~24), even less than the heat-stressed wild-type plants (~37) (Fig. 2M, O and Q, $P < 0.05$). On the other hand, the *rad51* mutant showed similar number of γH2A.X foci (~119) as in the wild-type plants indicating for normal DSB formation (Fig. 2M and R). In addition, the number of γH2A.X foci in the heat-stressed *rad51* mutant was lowered to a same level (~46) as in the heat-stressed wild-type plants (Fig. 2M and S). Taken together, these data supported that the suppressed chromosome fragmentation phenotype in heat-stressed *syn1* and *rad51* plants was owing to lowered DSB formation; additionally, it suggested that the heat stress reduces DSB formation independently of the organization of SYN1-mediated chromosome axis.

Heat stress does not affect SYN1-mediated chromosome axis

Since DSB formation relies on the normal construction of SYN1-mediated chromosome axis

211 (Lambing et al., 2020b), we checked whether the heat stress-interfered DSB formation was
212 due to affected SYN1 function by performing immunostaining of SYN1. Under control
213 temperature, SYN1 signals on the zygotene and pachytene chromosomes appeared linear
214 configuration in the wild-type plants (Supplement Fig. S4A and B), while no SYN1 foci was
215 detected in the *syn1* mutant (Supplement Fig. S4C). After heat stress, we observed that the
216 loading of SYN1 on both the zygotene and pachytene chromosomes was not influenced
217 (Supplement Fig. S4D and E), indicating that the high temperature does not target the
218 formation of SYN1-mediated chromosome axis. At the same time, we found that SYN1
219 accumulated normally on the zygotene chromosomes of *spo11-1-1* plants incubated under
220 both control and high temperature conditions (Supplement Fig. S4F and G). These data
221 suggested that the heat stress and the resultant reduction of DSB formation do not affect the
222 organization of SYN1-mediated axis.
223
224 **Heat stress induces pre-mature destabilization of axial element of synaptonemal**
225 **complex**
226
227 Construction of synaptonemal complex (SC) is required for homologous synapsis and
228 recombination (Higgins et al., 2005; Sanchez-Moran et al., 2007). To determine whether heat
229 stress inhibits CO by disrupting SC formation, we first looked at the axial structure of SC by
230 monitoring the localization of axis-associated ASY1 proteins. In leptotene-staged PMCs of
231 wild-type Col-0 plants incubated under control temperature, ASY1 foci displays punctate
232 configuration, and form a linear shape at early zygotene (Fig. 3A and B). At middle zygotene,
233 ASY1 foci are fully associated with the entire chromosomes at the lateral axis region (Fig.
234 3C). At late zygotene and early pachytene, when most homology are paired, ASY1 starts to
235 disassociated with some chromosome regions (Fig. 3D and E). Thereafter at middle pachytene,
236 when homologous chromosomes are fully synapsed, ASY1 signals reduce further and
237 disappear at late pachytene (Fig. 3F and G). After heat stress, we found that sparse and
238 punctate ASY1 foci occurred on both leptotene-, zygotene- and pachytene-staged
239 chromosomes (Fig. 3H and I, K-N). Interestingly, we can still find some middle zygotene
240 cells with normal ASY1 loading (Fig. 3J). These findings indicated that heat stress partially
241 induces pre-mature destabilization of ASY1-associated axial element of SC.
242
243 **Heat stress-induced ASY1 destabilization relies on the presence of SYN1 but not DSB**
244 **formation**
245
246 We wondered whether the compromised DSB formation and the interfered construction of
247 ASY1-associated axial element were independent issues impacted by the heat stress. To this
248 end, we analyzed ASY1 loading in heat-stressed *spo11-1-1* mutant plants. Under control
249 temperature, ASY1 configuration in *spo11-1-1* plants displayed normal as in wild-type plants
250 (Fig. 4A and B), indicating that the construction of ASY1-medited lateral element of axis does
251 not rely on DSB formation. Supportively, ASY1 signals on heat-stressed *spo11-1-1*
252 chromosomes exhibited dotted foci as in the heat-treated wild-type plants (Fig. 4E and F). As
253 the construction of lateral element of axis relies on functional SYN1 (Lambing et al., 2020b),
254 we then checked whether heat-interfered ASY1 loading is SYN1-dependent. As what has

been known, the *syn1* mutants has defective axial element structure indicated by the incomplete and/or fragmented ASY1 signals (Fig. 4C) (Lambing et al., 2020b). After heat stress, however, we didn't find punctate ASY1 foci in the heat-stressed *syn1* plants (Fig. 4G). This finding hinted that the heat stress influences lateral element of axis depending on the presence of SYN1.

Heat stress disrupts central element of synaptonemal complex

The ZYP1-dependent central element of SC is required for homology synapsis and recombination (Barakate et al., 2014; Higgins et al., 2005). To determine whether heat-induced univalent formation is (or at least partially) caused by impaired homolog synapsis, we performed immunolocalization of AtZYP1A in heat-stressed wild-type PMCs. In control plants, ZYP1 foci start to form linear configuration at zygotene, and are fully associated with the central element of SC at pachytene when homology synapsis is accomplished (Fig. 5A and D). In contrast, the ZYP1 signals on heat-stressed zygotene and pachytene chromosomes displayed dotted and/or fragmented foci (Fig. 5B and C, E and F). The ZYP1 assembly defects suggested that the heat stress has a serious impact on SC-based homologous synapsis.

As homologous synapsis also requires normal DSB formation (De Muyt et al., 2007; Grelon et al., 2001; Stacey et al., 2006), we then questioned whether the impacted construction of central element of SC was caused by the suppressed DSB formation. We observed that the *spo11-1-1* mutant failed to form linear ZYP1 foci but exhibited dotted signals representing interfered homology synapsis due to lack of DSB formation (Fig. 5G). After heat stress, however, unlike the wild-type plants that always showed dotted ZYP1 foci, no ZYP1 signal was observed in the *spo11-1-1* mutant (Fig. 5H). This data suggested that the heat stress can influences homology synapsis via a direct impact on ZYP1-dependent SC assembly.

Heat stress interferes with DMC1-mediated MR

DMC1 is required for MR-specific DSB repair (Da Ines et al., 2013; Kurzbauer et al., 2012; Sanchez-Moran et al., 2007), we wondered whether heat stress affects MR by inducing DMC1 dysfunction. We generated a novel anti-AtDMC1 antibody, which showed specific to AtDMC1 with no DMC1 foci detected in an *atdmc1* mutant (Supplement Fig. S5) (Sanchez-Moran et al., 2007), suggesting that the antibody is reliable. We found that in the wild-type plants the DMC1 number is significantly lowered by the high temperature (~18) (Fig. 6A, B and D), suggesting that heat stress has an impact on DMC1-mediated MR. Since SYN1-mediated axis formation is required for normal loading of DMC1 on chromatin (Lambing et al., 2020b), we then analyzed the impact of *SYN1* dysfunction on DMC1 in response to heat stress. We found that as reported, the *syn1* mutant has significantly less DMC1 on zygotene chromosomes compared with wild-type plants (~56) (Fig. 6A and C). After heat stress, the DMC1 foci decreased further in the *syn1* plants (~13) (Fig. 6A and E). This data suggested that heat stress may affect DMC1 independently of the SYN1-mediated axis construction.

Dynamics of DSB and DMC1 foci under increase of temperature

It has been reported that a mild high temperature condition at 28°C promotes MR rate through type-I pathway of CO formation independently of altering DSB formation in Arabidopsis (Lloyd et al., 2018; Modliszewski et al., 2018). Under a further elevated temperature condition (32°C), however, univalents are formed indicating for a lowered MR frequency (De Storme and Geelen, 2020). We therefore hypothesized whether interfered CO formation at 32°C is also attributed to an influenced DSB formation as the case at 36-38°C. The number of γH2A.X foci on zygotene chromosomes of wild-type Col-0 plants grown at 20°C, 28°C and 32°C was quantified. In line with the previous studies, the number of γH2A.X foci was not significantly altered at 28°C (~101) compared with 20°C (~118) (Fig. 7A-C, $P > 0.05$) (Modliszewski et al., 2018). However, plants treated by 32°C displayed a significantly reduced number of γH2A.X foci (~44) (Fig. 7A and D). This suggested that the univalent formation at 32°C probably also results from a compromised DSB generation. We also examined the DMC1 dynamics under the different high temperature conditions, and we found that the number of DMC1 foci kept stable (Fig. 7E, F-H, $P > 0.05$), indicating that a mild increase of temperature (around 32°C) does not influence DMC1-mediated MR.

Expression pattern of meiosis-related genes under cold and heat stresses

To address whether temperature alterations influence MR via modulated expression of meiotic genes, we performed transcriptome study on meiosis-staged flower buds from Col-0 plants stressed by 4°C, which is able to induce meiotic restitution (De Storme et al., 2012; Liu et al., 2018), and/or by a moderate high temperature (32°C) that can cause defects in both meiotic recombination and later meiotic stages (De Storme and Geelen, 2020), respectively (data not shown). From our data set, we picked up 108 genes which are involved, or play crucial roles in Arabidopsis male meiosis (Fig. 8A; Supplement File S2 and S3). By setting the significance level as $P < 0.05$, we found that most of the meiosis-related genes (61 genes) were downregulated and only 19 genes showed increased transcript level under 32°C (Fig. 8B; Supplement File S2). Among the 100 genes that showed significantly altered expression, only 4 genes including *SYN1* were upregulated and 31 genes were downregulated under both the cold and heat stresses (Fig. 8B; Supplement File S2). The selected 108 genes were cataloged into seven groups according to their function in meiosis (Fig. 8A). In the catalog of DSB formation, the expression of the key DSB catalyzers *SPO11-1* and *SPO11-2* were not altered under the heat stress (Fig. 8A; Supplement File S2). However, *PRD1*, *2* and *3*, which are key components of DSB formation machinery complex (Kim and Choi, 2019), were downregulated by the high temperature (Fig. 8A; Supplement File S2). Remarkably, among the genes required for SC formation, the expression of both *ZYP1A* and *ZYP1B* were lowered (Fig. 8A; Supplement File S2). The expression of axial-related elements *ASY3* and *ASY4* were reduced, but *ASY1* was not changed (Fig. 8A; Supplement File S2). *PCH2*, which acts in axis remodeling (Lambing et al., 2015), was downregulated under the high temperature (Fig. 8A; Supplement File S2). Genes involved in DSB repair; e.g. *RAD51*, *RAD51C*, *HOP2*, *MND1* and *MRE11* (Puizina et al., 2004; Su et al., 2017; Uanschou et al., 2013), showed reduced

transcript levels under heat stress, which, however, was not the case for recombinase *DMC1* (Fig. 8A; Supplement File S2). We also observed that the *Cyclin-dependent kinase G1* (*CDKG1*), which plays a role in processing of recombination intermediates and CO formation (Nibau et al., 2020), was upregulated by the high temperature but was not altered by the cold stress (Fig. 8A; Supplement File S2). This supported the notion that *CDKG1* is required for MR under high temperature (Zheng et al., 2014).

To consolidate the impact of heat stress on the expression of genes with a key role in MR, we examined expression of *SPO11-1*, *SYN1*, *ASY1*, *ZYP1*, *DMC1*, *RAD51*, *Ataxia-Telangiectasia Mutated* (*ATM*) and *Rad3-Related* (*ATR*) in meiosis-staged flower buds from Col-0 plants stressed by 36-38°C for 24 h using quantitative RT-PCR (qPCR) (Supplement Fig. S6). Arabidopsis heat shock sensor *HSFA1a* was used as the positive control (Yoshida et al., 2011), which showed 1.71-fold increased expression level under heat stress (Supplement Fig. S6A, $P < 0.05$). We found that except for *ZYP1A* and *ATR*, which displayed same expression level as under control temperature (Supplement Fig. S6E and I, $P > 0.05$), the selected genes assayed by qRT-PCR exhibited same variation patterns under 36-38°C as the transcriptome analysis under 32°C (Supplement Fig. S6B, C, D, F, G and H).

Increase of temperature influences the landscape of DNA methylation on chromatin

The landscape of both DSBs and CO highly correlates with methylation status of chromatin (Choi et al., 2018; He et al., 2017; Lambing et al., 2020b; Underwood et al., 2018; Yelina et al., 2015). To test whether affected distribution of CO under increased temperature is caused by variation in DNA methylation landscape (De Storme and Geelen, 2020), we performed immunolocalization of methylated cytosines in wild-type Col-0 plants using an anti-5-methylcytosine (5mC) antibody. Under control temperature, 5mC foci were found to be enriched at heterochromatin regions on leptotene, zygotene and pachytene chromosomes (Fig. 9A-D), which was in line with the previous report (Oliver et al., 2016). Under 32°C, however, we found that 5mC signal showed increased or decreased enrichment at some euchromatin or heterochromatin regions on the prophase chromosomes, respectively (Fig. 9E-I, see white arrows). Similar alterations were observed in plants stressed by 36-38°C (Fig. 9J-N, see white arrows). These observations suggested that the increase of temperature has an impact on the occurrence and/or distribution of DNA methylation on chromatin during MR.

Discussion

The influential pattern of temperature elevation on MR

MR in plants is sensitive to variations of environmental temperature (Bomblies et al., 2015; Liu et al., 2019; Modliszewski and Copenhaver, 2017). Lloyd et al. proposed that the MR rate of Arabidopsis under different temperature conditions within fertility-tolerable range displays a 'U-shape' pattern, in which both decrease (8°C) and increase (28°C) of temperature promote occurrence of MR (Lloyd et al., 2018). A similar pattern was found in wheat incubated between 10~26°C (Coulton et al., 2020), suggesting that within fertility threshold, elevation of temperature has a positive impact on MR frequency which may be conserved between dicots and monocots. It was recently evidenced that at 32°C Arabidopsis plants produce univalents and undergo non-homologous interactions, indicating that at this temperature point CO formation has been interfered at a certain level (De Storme and Geelen, 2020). In this study, we show that an extreme higher temperature over fertility-tolerable threshold (36-38°C) fully inhibits CO formation and MR in Arabidopsis. Therefore, it is likely that there is a small temperature interval between 28 to 32°C where MR occurrence reaches peak in Arabidopsis. In Arabidopsis, moderately elevated temperature promotes MR via enhanced activation of type-I CO formation pathway instead of by influencing DSB formation (Lloyd et al., 2018; Modliszewski et al., 2018). Similarly, in *Schizosaccharomyces pombe*, MR rate is moderately changed but DSB formation is not influenced under temperature conditions within the fertile range between 16 to 33°C (Brown et al., 2019). We here show that in Arabidopsis, together with a decrease and/or abolishment of COs (Supplement Fig. S1) (De Storme and Geelen, 2020), DSB formation is significantly reduced at and/or above 32°C (Fig. 1 and 7). Supportively, we observed that at 36-38°C chromosome fragmentation in the *syn1* and *rad51* mutants was partially suppressed, and both the heat-stressed mutants with lowered DSB formation were able to produce univalents (Fig. 2). We thus demonstrate that beyond a tolerable temperature point, increase of temperature reduces SPO11-dependent DSB generation in Arabidopsis.

We found that the expression of DSB generation catalyzers *SPO11-1* and *SPO11-2* kept stable under high temperatures (Fig. 8A; Supplement Fig. S6). However, the key elements of DSB formation complexes; i.e. *PRD1* and *PRD3*, which are required for loading of other DSB formation proteins on chromatin (Carballo et al., 2008; De Muyt et al., 2007), were downregulated by the high temperature (Fig. 8A). The heat stress-compromised DSB formation is therefore not likely to be caused by a lowered abundance of SPO11 proteins, but could be due to its loading on DSB generation sites. Arabidopsis plants with defect in DSB generation have largely suppressed CO formation, and produce univalents instead of bivalents (De Muyt et al., 2007; Grelon et al., 2001; Hartung et al., 2007; Stacey et al., 2006), the heat stress-impaired occurrence of CO is therefore probably due to the reduction of DSBs. In *S. cerevisiae*, it has been reported that DSB repair defect (manifested by calculated gene conversion rate) in the *rad55* and/or *rad57* mutants is more severe at lower temperatures (Pohl and Nickoloff, 2008). This suggests that increase of temperature may reduce DSB

formation in *S. cerevisiae*, either, which may be a conserved phenomenon among eukaryotes. Based on these findings, we propose that there probably exists a homeostasis between a positive impact of high temperature on type-I CO formation machineries and a negative influence on DSB formation in Arabidopsis: a limited temperature elevation within the tolerable range of DSB formation (e.g. 28°C) has a positive effect on activation of ZMM proteins and subsequently promotes the occurrence of interfering-sensitive COs. However, when the temperature continuously increases reaching a point when SPO11-dependent DSB formation starts to be impaired (starting from 32°C), MR rate decreases and is fully inhibited at 36-38°C (Fig. 10).

SC assembly is another prominent target by high temperature stimulus

It is considered that variations of temperature influence MR via a predominant impact on the organization of SC (Morgan et al., 2017). In support of this, De Storme et al. revealed that at 32°C ASY1 foci appear normal but linear configuration of ZYP1 on pachytene chromosomes is interrupted in Arabidopsis (De Storme and Geelen, 2020). Also, in barley, a moderate high temperature causes a slight but significant decrease of CO formation by affecting ZYP1-dependent SC assembly (Higgins et al., 2012). Here, we show that the SYN1-mediated axis formation is not sensitive to the 36-38°C high temperature (Supplement Fig. S4), however, the ASY1-associated axial element of SC is partially influenced (Fig. 3), and the ZYP1-dependent central element of SC is severely disrupted by the heat stress (Fig. 5). These findings indicate that ZYP1-dependent organization of transverse filaments (TFs) between the chromosome axes is the main target of heat stress. Considering the essential requirement of SC structure to successful CO formation (Higgins et al., 2005), disassembly of SC and the resultant failed homology synapsis is likely to be another prominent reason besides lowered DSB formation for the inhibited MR under heat stress. This possibility is supported by the observation that the number of DSBs are lowered to a similar level at 32°C and 36-38°C (Fig. 1 and 7), but ZYP1 loading is not completely disrupted with CO rate partially retained at 32°C (De Storme and Geelen, 2020).

Our transcriptome study and qRT-PCR showed that the transcript of *ASY1* is not changed under the high temperatures (Fig. 8A; Supplement Fig. S6), suggesting that the high temperatures influence ASY1-mediated axial element construction not by modulating the expression of *ASY1*. The loading of ASY1 on chromatin requires the presence and function of ASY3 (Ferdous et al., 2012; Lambing et al., 2020a), the localization on chromosomes of which in turn relies on axis-associated protein ASY4 (Chambon et al., 2018). We found that the expression of ASY3 and ASY4 are downregulated at 32°C (Fig. 8A), suggesting that the irregular ASY1 assembly under heat stress could be due to its compromised loading to chromatin caused by the reduced ASY3 and ASY4 abundance. The phosphorylation of ASY1 catalyzed by the cyclin-dependent kinase Cdk1/Cdk2 homolog CDKA ;1 is required for its self-polymerization on chromosome axis through ASY3 (Yang et al., 2019). We show that the expression of CDKA ;1 is not influenced under high temperature (Fig. 8A), implying that disassembly of ASY1 may not be owing to its altered phosphorylation status. However, we cannot exclude the possibility that the transcript of CDKA ;1 is lowered at 36-38°C, or

465 alternatively, the affinity of CDKA ;1 to ASY1 is indeed interfered. Moreover, the formation
466 of ASY1-associated axis relies on the key axis component SYN1 (Lambing et al., 2020b), and
467 we found that the heat stress does not induce dotted ASY1 configuration in the *syn1* mutant
468 (Fig. 4), suggesting that heat stress disturbs the assembly of ASY1 requires the presence of
469 SYN1. More molecular studies are needed to decipher the role of SYN1 in mediating the
470 response of ASY1 to temperature increase.
471
472 Arabidopsis plants with loss of ASY1 exhibit normal number of DSB and axis structuring, but
473 have impaired homologous synapsis manifested by disrupted ZYP1 configuration (Ferdous et
474 al., 2012; Sanchez-Moran et al., 2007). Therefore, heat stress-induced DSB reduction is not
475 caused by the disorganization of ASY1-mediated axis. In addition, since we can find many
476 zygotene cells with normal ASY1 loading but did not see any cells with complete ZYP1
477 signal on pachytene chromosomes, failed homologous synapsis under heat stress is not likely
478 to be mainly owing to the interfered ASY1 function. Nevertheless, the normal localization of
479 ASY3 is required for DSB formation and ZYP1-dependent homology synapsis (Chambon et
480 al., 2018; Ferdous et al., 2012; Sanchez-Moran et al., 2007), hence the lowered ASY3 and
481 ASY4 transcripts may also contribute to the defects of DSB formation and the ZYP1
482 assembly. Examining the localization of ASY3 and ASY4 on heat-stressed chromatins thus
483 would help to clarify this hypothesis.
484
485 **DMC1-dependent MR is sensitive to high temperature**
486
487 The recombination-specific DSB repair is catalyzed by recombinase DMC1 (Cloud et al.,
488 2012; Kurzbauer et al., 2012; Sanchez-Moran et al., 2007). In wheat, heat stress lowers CO
489 formation and this impact is more pronounced in the *tadmc1* mutant, suggesting that DMC1 is
490 a target of high temperature in affecting MR (Draeger et al., 2019). In *Schizosaccharomyces*
491 *pombe* it was proposed that recombinases involved in DSB processing are potential targets of
492 temperature stimulus (Brown et al., 2019). In our study, we observed that the DMC1 foci on
493 zygotene chromosomes were reduced in heat-stressed PMCs indicating for an interfered
494 DMC1-mediated DSB maturation. This finding supports that among species,
495 DMC1-dependent MR is a sensitive process during MR in response to high temperature. We
496 did not detect a lowered expression of *DMC1* under heat stress (Fig. 8A; Supplement Fig. S6),
497 suggesting that high temperature may reduce DMC1 foci at a post-transcription level; e.g. by
498 modulating the affinity of DMC1 to chromatin. Indeed it has been considered that heat stress
499 interferes with MR by directly influencing the activity of proteins involved in DSB processing
500 and/or CO formation (Börner et al., 2004; Hotta et al., 1988; Smith et al., 2003).
501 SYN1-mediated axis construction is required for the normal function of DMC1 (Lambing et
502 al., 2020b). We found that the accumulation of SYN1 on chromatin is not affected by heat
503 stress, and the number of DMC1 foci in heat-stressed wild-type and *syn1* plants decreases to a
504 same level (Supplement Fig. S4; Fig. 6), hinting that increase of temperature may affect
505 DMC1-dependent MR independently of SYN1-mediated axis formation. However, it cannot
506 be excluded that the interfered loading of DMC1 on chromatin is caused by the compromised
507 ASY1 and/or ASY3 function (Ferdous et al., 2012; Sanchez-Moran et al., 2007). On the other
508 hand, the accumulation of DMC1 on chromatin depends on RAD51 (Cloud et al., 2012;

Vignard et al., 2007), it thus may be the case that the 36-38°C high temperature affects the stability of DMC1-ssDNA nucleoprotein filament via influenced transcript of RAD51 (Fig. 8A; Supplement Fig. S6). Moreover, since the loading of DMC1 requires normal DSB formation (De Muyt et al., 2007), the reduction of DMC1 may at least partially be owing to a compromised DSB generation. However, we found that the DSB foci was lowered at 32°C, which was not the case for DMC1 (Fig. 7). This implies that the loading of DMC1 has a higher threshold than DSB formation against high temperature. Therefore, it is possible that the high temperature imposes a direct impact on DMC1 in addition to the interfered SPO11-dependent DSB formation.

DNA methylation plays a potential role in altered CO landscape under high temperature

Environmental temperatures influence the landscape of CO in multiple species (Coulton et al., 2020; De Storme and Geelen, 2020; Zhang et al., 2017). The number of DSBs has an impact on the distribution of CO in Arabidopsis (Xue et al., 2018). The affected DSB formation at higher temperature conditions (e.g. 32°C) thus may contribute to the alterations in the landscape of CO. On the other hand, the landscapes of both DSBs and CO are shaped by genomic features including epigenetic modification status/patterns of DNA and histone proteins (Choi et al., 2013; Choi et al., 2018; He et al., 2017; Underwood et al., 2018; Yamada et al., 2017), which are targets of temperature stimulus (Chang et al., 2020). We here showed that the DNA methylation status at euchromatin and/or heterochromatin regions of chromatin are changed upon the elevation of temperature (Fig. 9). The heat-induced reshape of CO landscape hence could partially be owing to the variation of DNA methylation distribution on chromatin. Examination the landscape of DSB and/or CO in heat-stressed mutants defective for *de novo* and/or maintenance of DNA methylation; e.g. *drm1 drm2 cmt3* and *met1* (Zhang et al., 2006) would contribute to the understanding the association of DNA methylation and MR in response to temperature alterations.

Supplemental Files

The following files are available in the online version of this article.

Supplement Figure S1. DAPI-staining of meiotic chromosomes in heat-stressed wild-type Col-0 plants.

Supplement Figure S2. Meiotic products of heat-stressed wild-type Col-0 plants stained by orcein.

Supplement Figure S3. FISH analysis of chromosome dynamics in heat-stressed wild-type Col-0 plants.

Supplement Figure S4. SYN1-mediated chromosome axis appears normal under heat stress.

Supplement Figure S5. Immunolocalization of DMC1 in the *dmc1* mutant.

Supplement Figure S6. Expression of MR-related genes under 36-38°C heat stress.

Supplement Table S1. Primers used in this study.

Supplement File S2. Expression change of meiosis-related genes under cold and heaty stresses.

Supplement File S3. FPKM values of mRNA of the 108 meiosis-related genes obtained from 15 biological replicates for both the control, cold- and heat-stressed plants.

Supplement File S4. Identity of 100 meiosis-related genes with their expression-change patten under cold and heat stresses.

Material and Methods

Plant materials and growth conditions

Arabidopsis thaliana ecotypes Columbia-0 (Col-0) and Wassilewskija (Ws) plants were used as wild-type plants. The *syn1-1* (SALK_137095) (Ws background), *rad51* (SAIL_873_C08) (Col-0 background), *spo11-1-1* (Ws background) (Grelon et al., 2001) and *dmc1* (SALK_056177) (Col-0 background) mutants were used in the study. Seeds were germinated in soil for 6-8 days and seedlings were transferred to soil and cultivated in growth chambers with a 16 h day/8 h night, 20°C, and 50% humidity condition. For temperature stress treatment, young flowering plants were transferred to a humid chamber with a 16 h day/8 h night and at 28, 32 and 36-38°C conditions for 24 h, respectively. All the treatment assays started from 8:00-10:00 AM. Meiosis-staged flower buds were fixed right away upon the finish of treatment.

Generation of antibodies

AtZYP1 (rabbit) and AtDMC1 (rabbit) antibodies were generated by GL Biochem, Shanghai, Ltd: www.glschina.com, by referring to (Yu et al., 2012). AtASY1 (rabbit) antibody was generated by Dr. Chunli Chen lab, Huazhong Agricultural University. Peptide antisera were raised in rabbits against the amino acid sequences of NCSQASQDRRGRKTS (AtASY1) conjugated to KLH. Purification of antibodies was performed using polypeptide affinity followed by Elisa test (> 1:32000).

Immunolocalization and fluorescence in situ hybridization (FISH)

Immunolocalization assays were performed by referring to (Chelysheva et al., 2010; Wang et al., 2014). Antibodies against ASY1 (rabbit), ZYP1 (rabbit), DMC1 (rabbit) and γH2A.X (rabbit) were diluted by 1:100; antibodies against SYN1 (rabbit) (Wang et al., 2020) and 5-Methylcytosine (Invitrogen, MA5-24694) was diluted by 1:500. The secondary antibodies, i.e. Goat anti-Rabbit IgG (H+L) Cross-Adsorbed Secondary Antibody Alexa Fluor 555 (Invitrogen, A32732) and Goat anti-Rabbit IgG (H+L) Highly Cross-Adsorbed Secondary Antibody Alexa Fluor Plus 488 (Invitrogen, A32731) were diluted by 1:400. FISH and used centromere-specific probes were referred to (Lei et al., 2020).

Transcriptomic Analysis

Total RNA was isolated from meiosis-staged flower buds of Arabidopsis Col-0 plants which

were incubated at 4°C, 20°C and 32°C, respectively. Fifteen biological replicates were used for each temperature treatment, and for each replicate, more than 20-30 plant individuals were pooled for sampling. Sequencing was performed using an Illumina NovaSeq 6000 instrument. Clean reads were obtained by removing reads containing adapter, reads containing ploy-N and low-quality reads from raw data using the in-house perl scripts. For quantification of the expressed abundance for genes, clean reads were mapped to the Arabidopsis reference genome (TAIR v10.0) using HISAT2 (v2.1.0) (Pertea et al., 2016) and genes were quantified by StringTie (v1.3.1) (Liao et al., 2014). Principal component analysis (PCA) based on K-means analysis of FPKM values of 45 samples showed that samples from different treatments of temperatures can be well separated. We calculated the average of FPKM values of 4°C, 20°C and 32°C, respectively. Based on the reported meiosis-related genes, the normalized expression of genes with Z-score for FPKMs is shown in the heatmap.

Quantitative RT-PCR (qRT-PCR)

Total RNA was isolated from meiosis-staged flower buds of Arabidopsis Col-0 plants grown under normal temperature conditions (20ºC) and after 36-38ºC treatment for 24 h, respectively. First-strand cDNA was synthesized using the PrimeScriptTM II 1st Strand cDNA Synthesis Kit (TAKARA, Kusatsu, Japan) according to the manufacturer's protocol. qRT-PCR was performed on a QuantStudio 1 Real-Time PCR System (Applied BiosystemsTM, Thermo Fisher Scientific) using the Applied BiosystemsTM PowerUpTM SYBRTM Green Master Mix (Thermo Fisher Scientific, Vilnius, Lithuania). The reaction mix was prepared with 10.0 µL PowerUpTM SYBRTM Green Master Mix, 0.4 µL 10 µM forward primer, 0.4 µL 10 µM reverse primer, 75 ng cDNA, and nuclease-free water up to a total volume by 20.0 µL. For both the control and heat stress conditions, three biological replicates were analyzed, and for each sample, three technical replicates for each targeted gene were performed. *EF1αA4* (At5g60390) was used as the reference gene (Parra-Rojas et al., 2019), and the relative expression fold-change was calculated using the Comparative CT method. Significance analysis was performed using the one-way ANOVA test, and significance level was set as 0.05. The used primers are listed in Supplement Table S1.

Microscopy

Fluorescence images were recorded using an Olympus IX83 inverted fluorescence microscope with a X-Cite lamp and a Prime BSI camera. Bifluorescent images and Z-stacks were processed using Image J. Brightness and contrast setting of pictures were adjusted using PowerPoint 2016.

Accession Numbers

Accession numbers of all genes studied in this work are: *SPO11-1* (AT3G13170), *ASY1* (AT1G67370), *ZYP1a* (AT1G22260), *ZYP1b* (AT1G22275), *SYN1* (AT5G05490), *DMC1* (AT3G22880), *RAD51* (AT5G20850), *ATM* (AT3G48190), *ATR* (AT5G40820), *HSFA1a*

(AT4G17750) and *EF1αA4* (At5g60390).

Conflict of interest

Nothing declared.

Funding

The research was supported by National Natural Science Foundation of China (32000245, to B.L.), Hubei Provincial Natural Science Foundation of China (2020CFB159, to B.L.), Fundamental Research Funds for the Central Universities, South-Central University for Nationalities (CZY20001, to B.L.), Fundamental Research Funds for the Central Universities, South-Central University for Nationalities (YZZ18007, to B.L.), Hubei Provincial Natural Science Foundation of China (2020CFB157 to Q.P.L.), and the Fundamental Research Funds for the Central Universities, South-central University for Nationalities (YZZ19007 to Q. P.L.).

Acknowledgement

We thank very much for the suggestions and comments from Dr. Wojtek Pawlowski (Cornell University) for this work. We appreciate Dr. Yingxiang Wang (Fudan University) for kindly sharing the *syn1*, *rad51*, *spo11-1-1* and *dmc1* mutants, and the anti-SYN1 antibody. We thank Dr. Yan He (China Agricultural University) very much for kindly sharing the anti-γH2A.X antibody. We thank Dr. Cong Wang (Fudan University) and Dr. Wenqing Shi (Institute of Genetics and Developmental Biology, Chinese Academy of Sciences) for the technical help on immunolocalization assays. Especially, we thank Mrs. Meirong Huang, Mrs. Manxiang Zhu, Mr. Donglin Liu, Mrs. Jiajia Zhao and Ms. Zipei Liu for the support during the occurrence of coronavirus COVID-19 global cases.

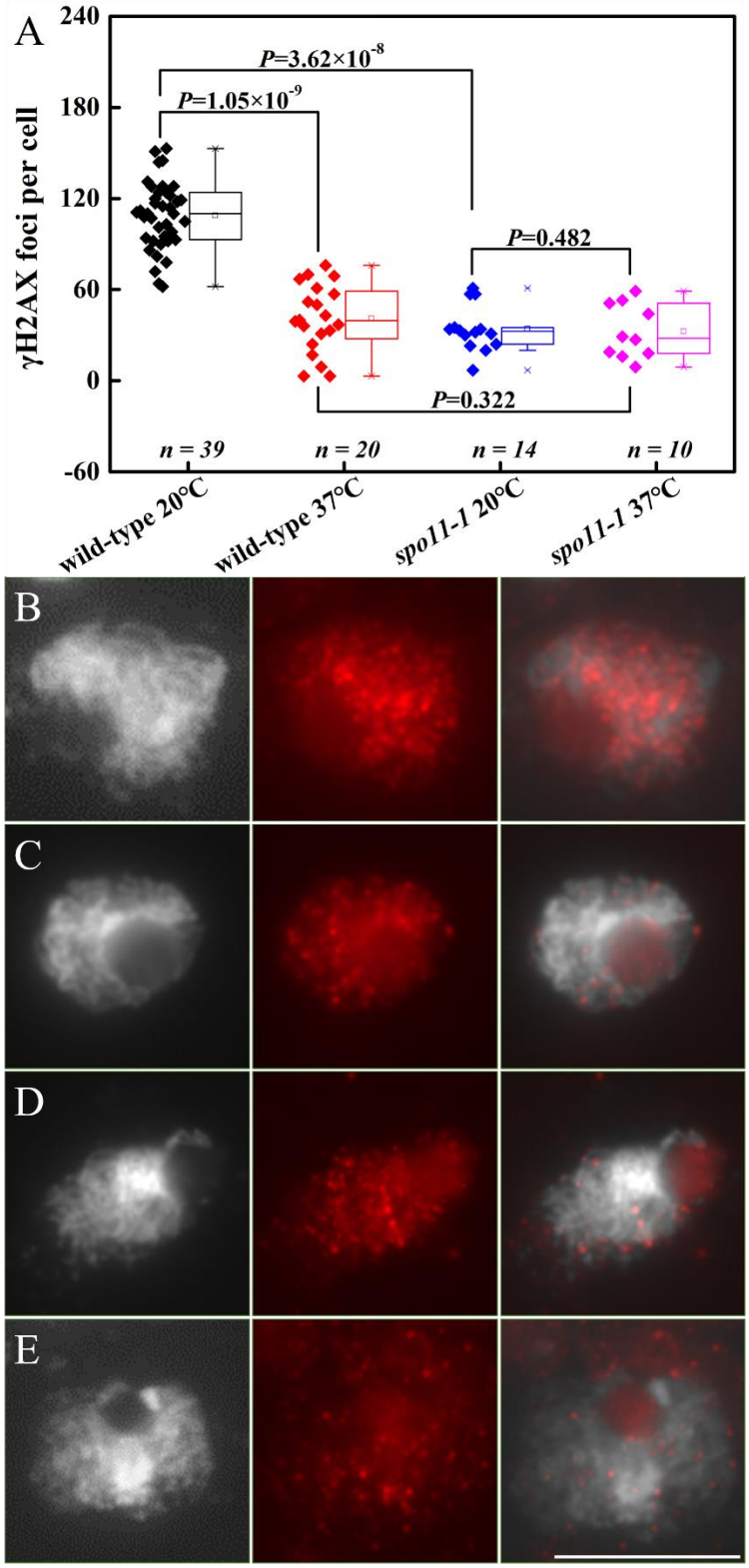

Figure 1. Immunolocalization of γH2A.X in heat-stressed wild-type Ws and *spo11-1-1* mutant plants. A, Graph showing the quantification of γH2A.X foci in wild-type and the *spo11-1-1* mutant under normal temperature and high temperature conditions. Two-side Mann-Whitney *U* test was performed. *n* indicates for the number of quantified cells. B and C, γH2A.X foci in wild-type (B) and *spo11-1-1* (C) plants under normal temperature conditions. D and E, γH2A.X foci in wild-type (D) and *spo11-1-1* (E) plants after heat stress. White: DAPI-stained chromosomes; Red: γH2A.X. Scale bar = 10 μm.

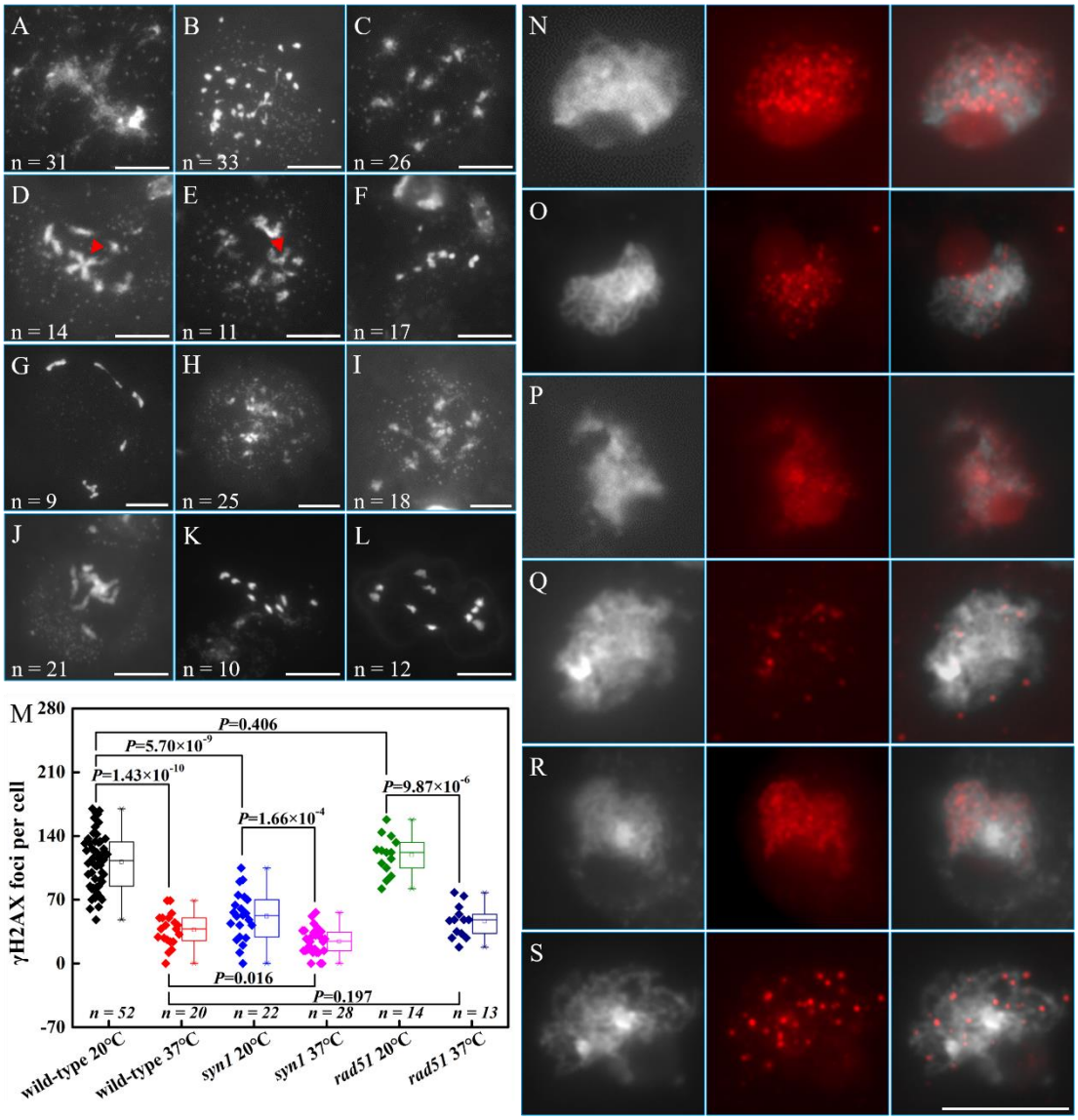

Figure 2. Heat stress partially suppresses chromosome fragmentation in the *syn1* and *rad51* mutants by lowering DSB formation. A and B, Diakinesis- (A) and metaphase I-staged (B) PMCs in the *syn1* mutant under normal temperature conditions. C-G, Diakinesis- (C-E) and metaphase I-staged (F and G) PMCs in the *syn1* mutant after heat stress. H and I, Diakinesis-staged PMCs in the *rad51* mutant under normal temperature conditions (H) and after heat stress (I). Red arrows indicate connections between the univalents. J-L, Diakinesis- (J) and metaphase I-staged (K and L) PMCs in the *spo11-1-1* mutant under normal temperature conditions. M, Graph showing the number of γH2A.X foci in heat-stressed wild-type Ws, *syn1* and *rad51* plants. Two-side Mann-Whitney *U* test was performed. *n* indicates for the number of cells used for quantification. N and O, Immunolocalization of γH2A.X in wild-type Ws under normal temperature conditions (N) and after heat stress (O). P and Q, Immunolocalization of γH2A.X in the *syn1* mutant under normal temperature conditions (P) and after heat stress (Q). R and S, Immunolocalization of γH2A.X in the *rad51* mutant under normal temperature conditions (R) and after heat stress (S). White: DAPI-stained chromosomes; Red: γH2A.X. Scale bars = 10 μm.

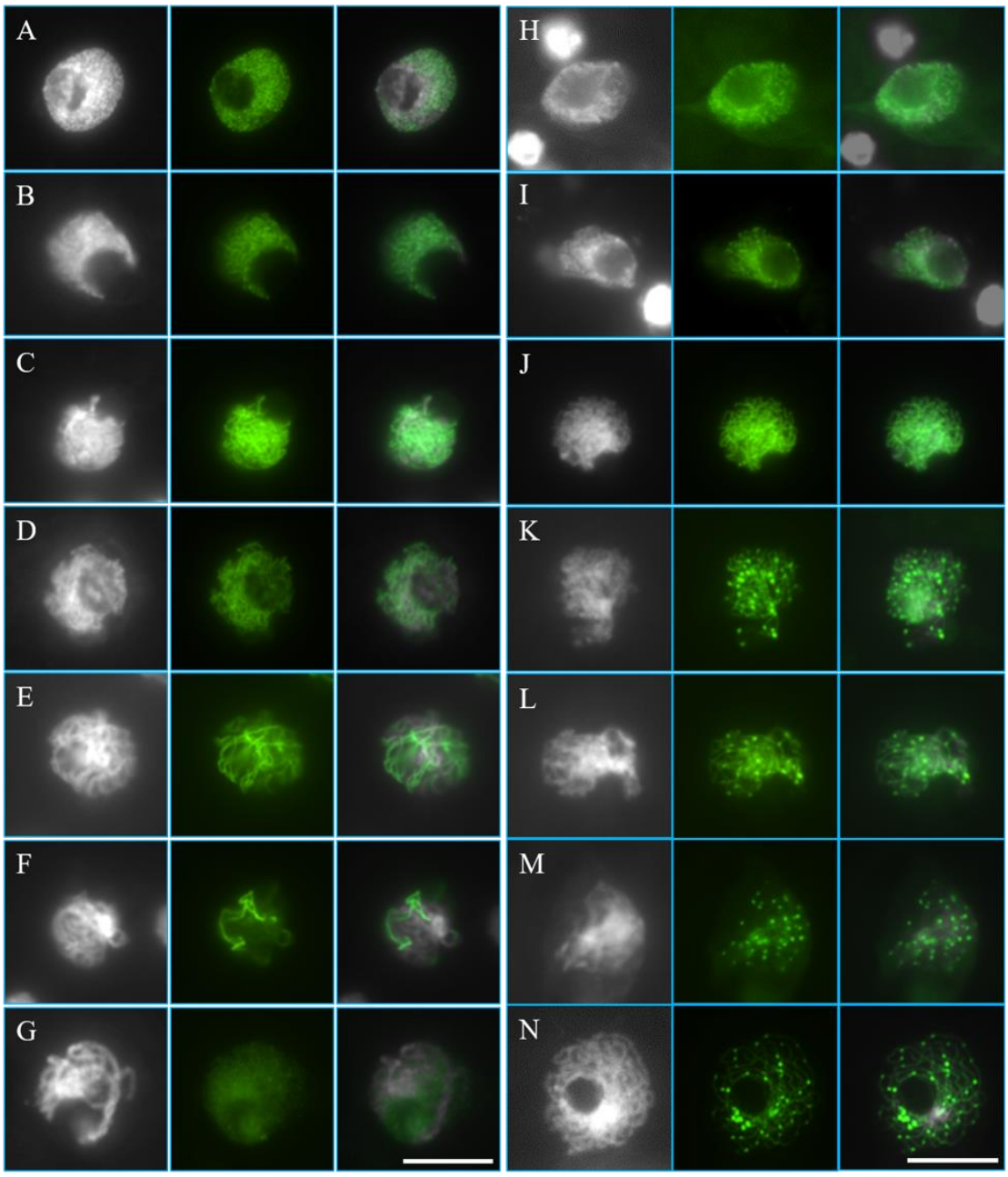

Figure 3. Immunolocalization of ASY1 in wild-type Col-0 plants under normal temperature and heat stress conditions. A-G, Chromosomes at leptotene (A), early zygotene (B), middle zygotene (C), late zygotene (D), early pachytene (E), middle pachytene (F) and late pachytene (G) under normal temperature conditions. H-N, Chromosomes at leptotene (H), early zygotene (I), middle zygotene (J-L), late zygotene (M) and middle pachytene (N) after heat stress. White: DAPI-stained chromosomes; Green: ASY1. Scale bars = 10 μm.

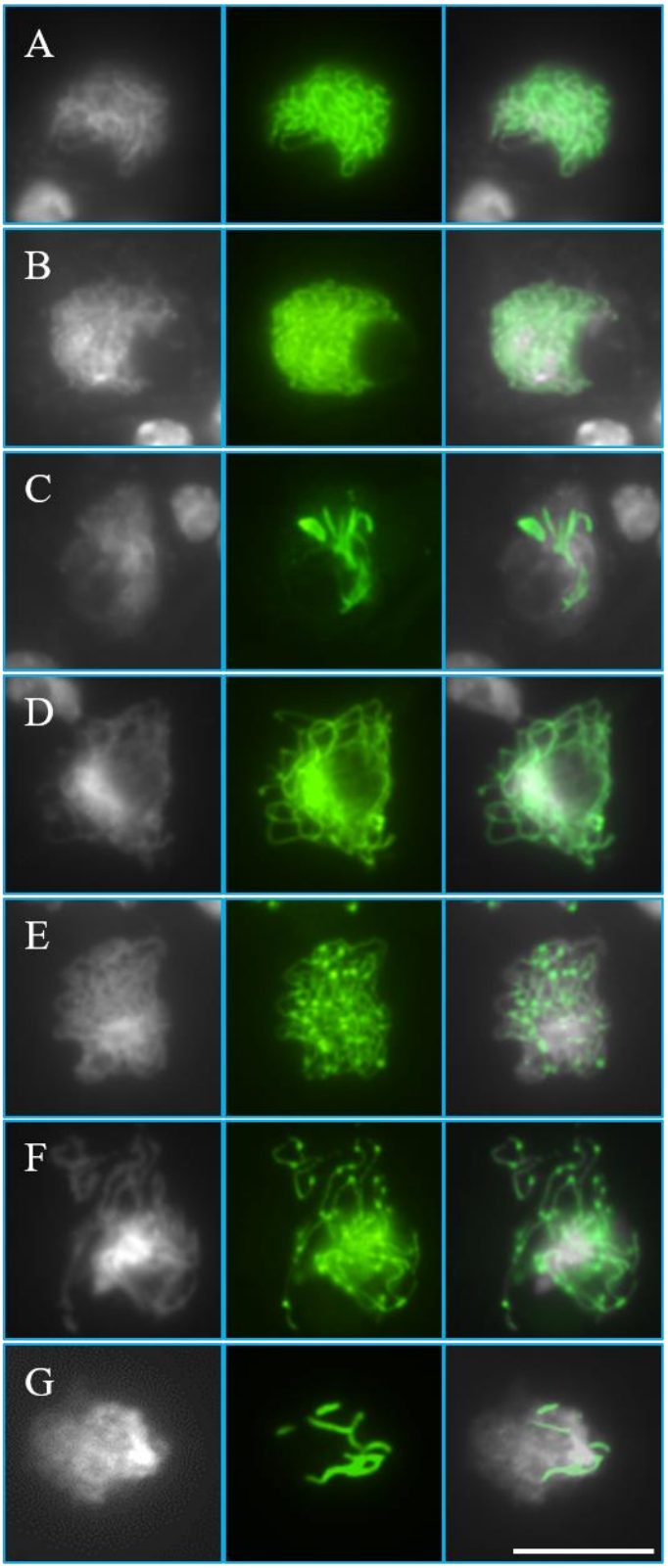

Figure 4. Immunolocalization of ASY1 in heat-stressed wild-type, *spo11-1-1* and *syn1* plants. A-C, ASY1 localization on zygotene chromosomes of wild-type (A), *spo11-1-1* (B) and *syn1* mutants (C) under normal temperature conditions. D-G, ASY1 localization on zygotene chromosomes of heat-stressed wild-type (D and E), *spo11-1-1* (F) and *syn1* mutants (G). White: DAPI-stained chromosomes; Green: ASY1. Scale bar = 10 μm.

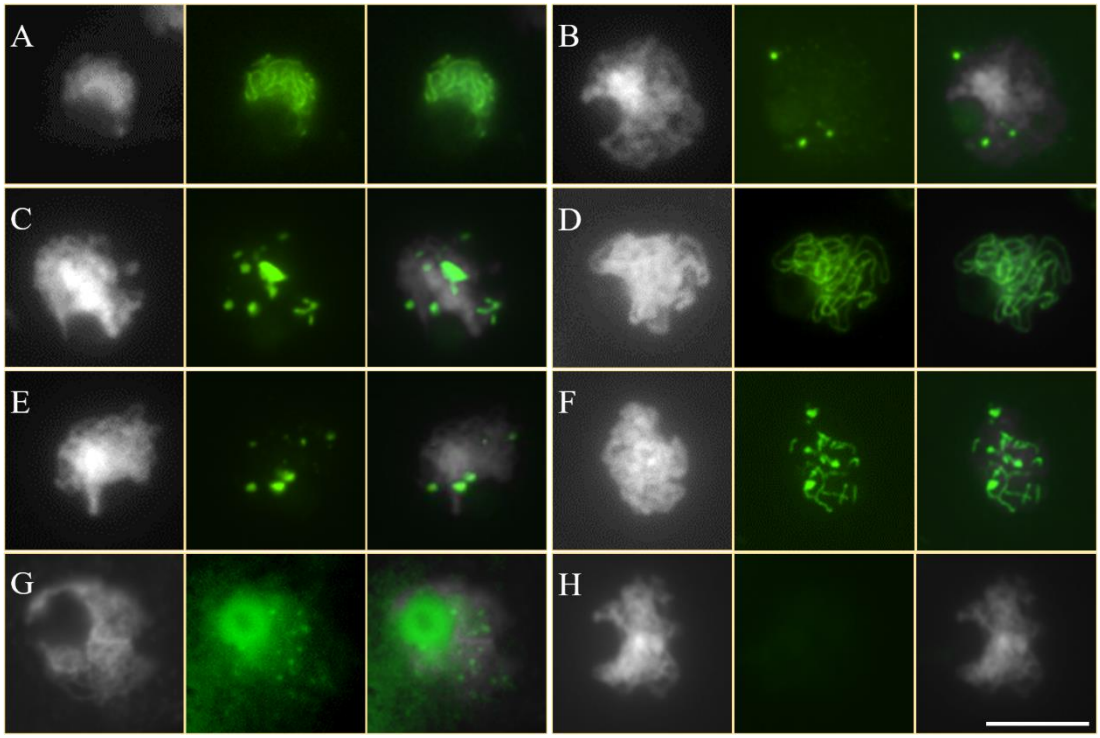

Figure 5. Immunolocalization of ZYP1 in heat-stressed wild-type and *spo11-1-1* mutant plants. A-C, ZYP1 localization on zygotene chromosomes of wild-type under normal temperature (A) and heat stress (B and C) conditions. D-F, ZYP1 localization on pachytene chromosomes of wild-type under normal temperature (D) and heat stress (E and F) conditions. G and H, ZYP1 localization on chromosomes of *spo11-1-1* mutant under normal temperature (G) and heat stress (H) conditions. White: DAPI-stained chromosomes; Green: ZYP1. Scale bar = 10 μm.

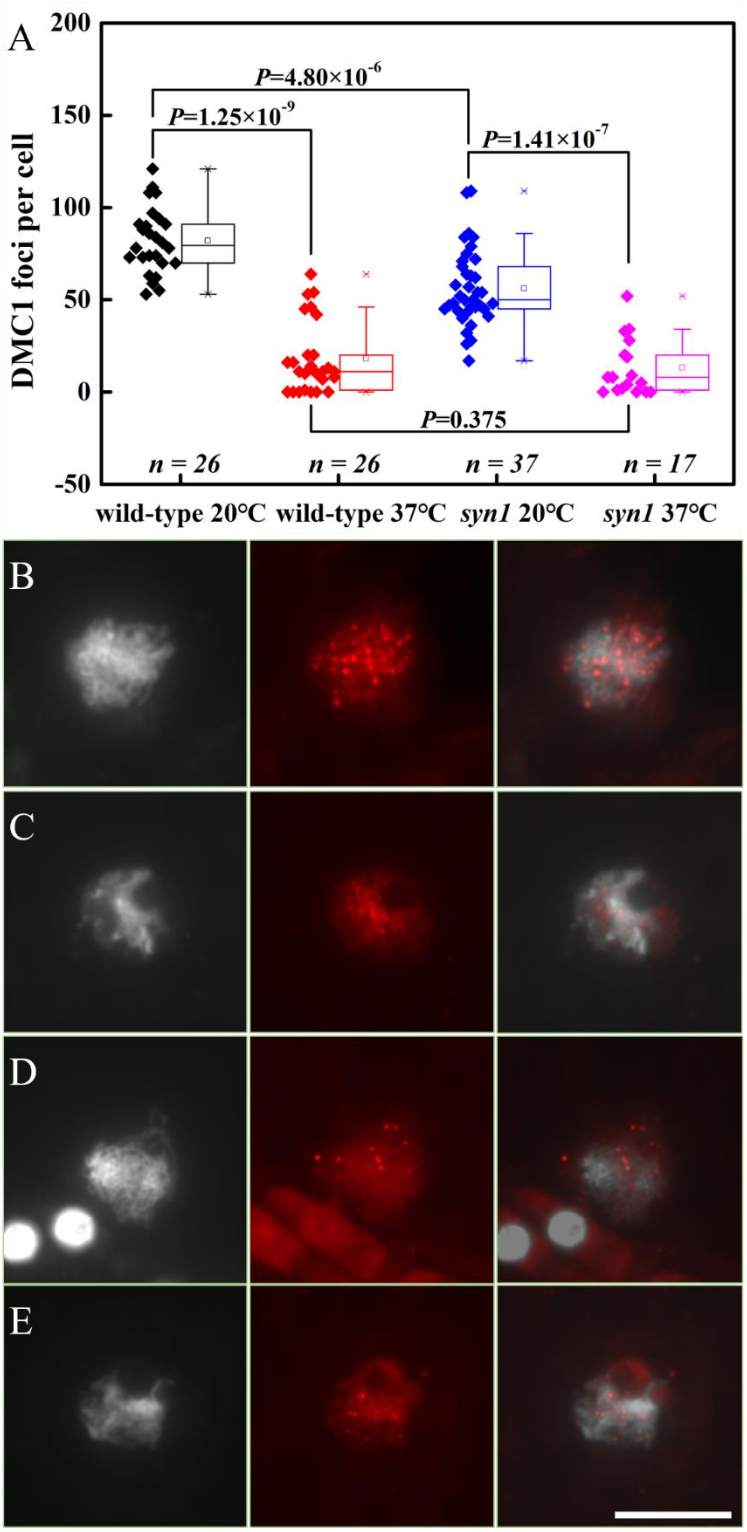

Figure 6. Immunolocalization of DMC1 in heat-stressed wild-type and *syn1* plants. A, Graph showing the number of DMC1 foci on zygotene chromosomes per PMC in wild-type and *syn1* plants under normal temperature and high temperature conditions. Two-side Mann-Whitney *U* test was performed. *n* indicates for the number of cells used for quantification. B and C, DMC1 localization on zygotene chromosomes in wild-type (B) and *syn1* (C) plants under normal temperature conditions. D-E, DMC1 localization on zygotene chromosomes in wild-type (D) and *syn1* (E) plants after heat stress. White: DAPI-stained chromosomes; Red: DMC1. Scale bar = 10 μm.

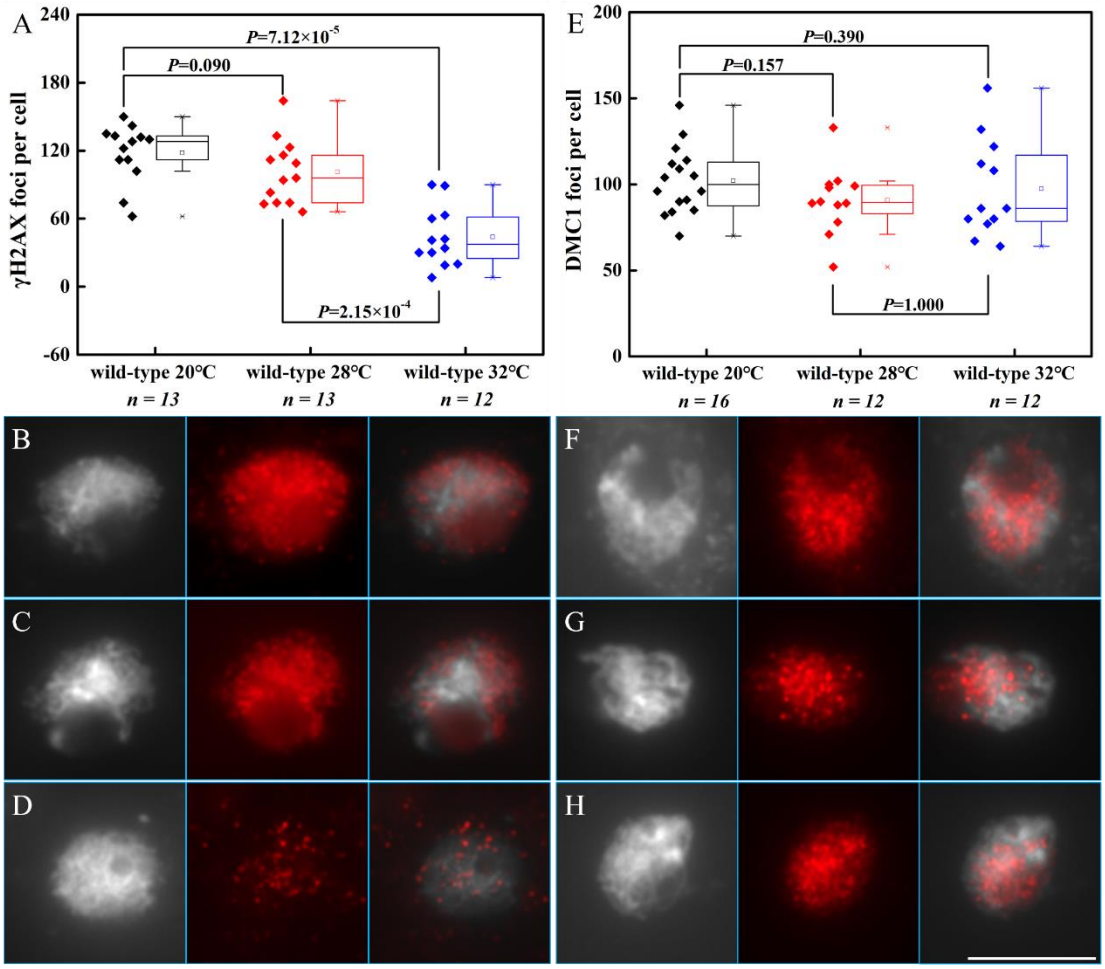

Figure 7. Immunolocalization of γH2A.X and DMC1 in wild-type Col-0 plants incubated at 20°C, 28°C and 32°C conditions. A, Graph showing the quantification of γH2A.X in wild-type Col-0 plants incubated at 20°C, 28°C and 32°C conditions. B-D, Localization of γH2A.X in wild-type Col-0 plants incubated at 20°C (B), 28°C (C) and 32°C (D) conditions. E, Graph showing the quantification of DMC1 in wild-type Col-0 plants incubated at 20°C, 28°C and 32°C conditions. F-H, Localization of DMC1 in wild-type Col-0 plants incubated at 20°C (F), 28°C (G) and 32°C (H) conditions. Two-side Mann-Whitney *U* test was performed. *n* indicates for the number of cells used for quantification. White: DAPI-stained chromosomes; Red: γH2A.X or DMC1. Scale bar = 10 μm.

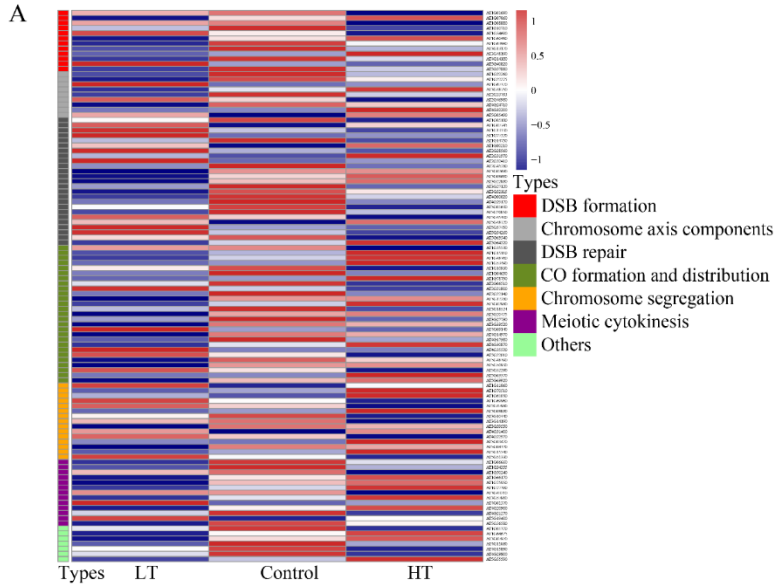

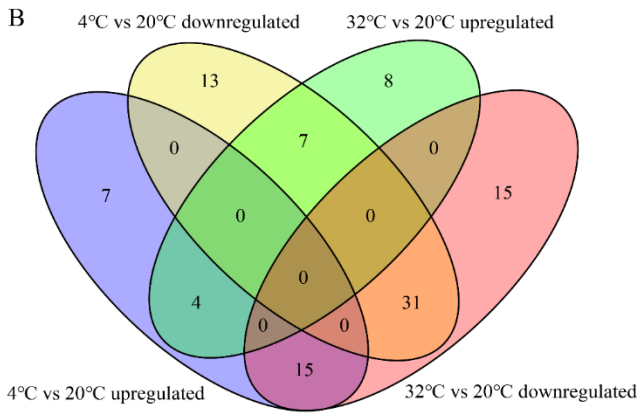

Figure 8. Expression pattern of meiosis-related genes under temperature stresses. A, Heatmap showing the expression patterns of 108 meiosis-related genes under low temperature (LT) (4°C), control temperature (20°C) and high temperature (HT) (32°C), respectively. The left column with different colors corresponds to seven catalogs including DSB formation, chromosome axis components, DSB repair, CO formation and distribution, chromosome segregation, meiotic cytokinesis and others. Colors represent the expression level of the selected genes indicated by scoring from −1 to 1 with red indicating a high expression level while blue indicating a low expression level. Gene IDs were presented at the right column. B, Venn diagram showing the significantly altered expression of the 100 meiosis-related genes under cold and heat stresses. Significance level was set as $P < 0.05$.

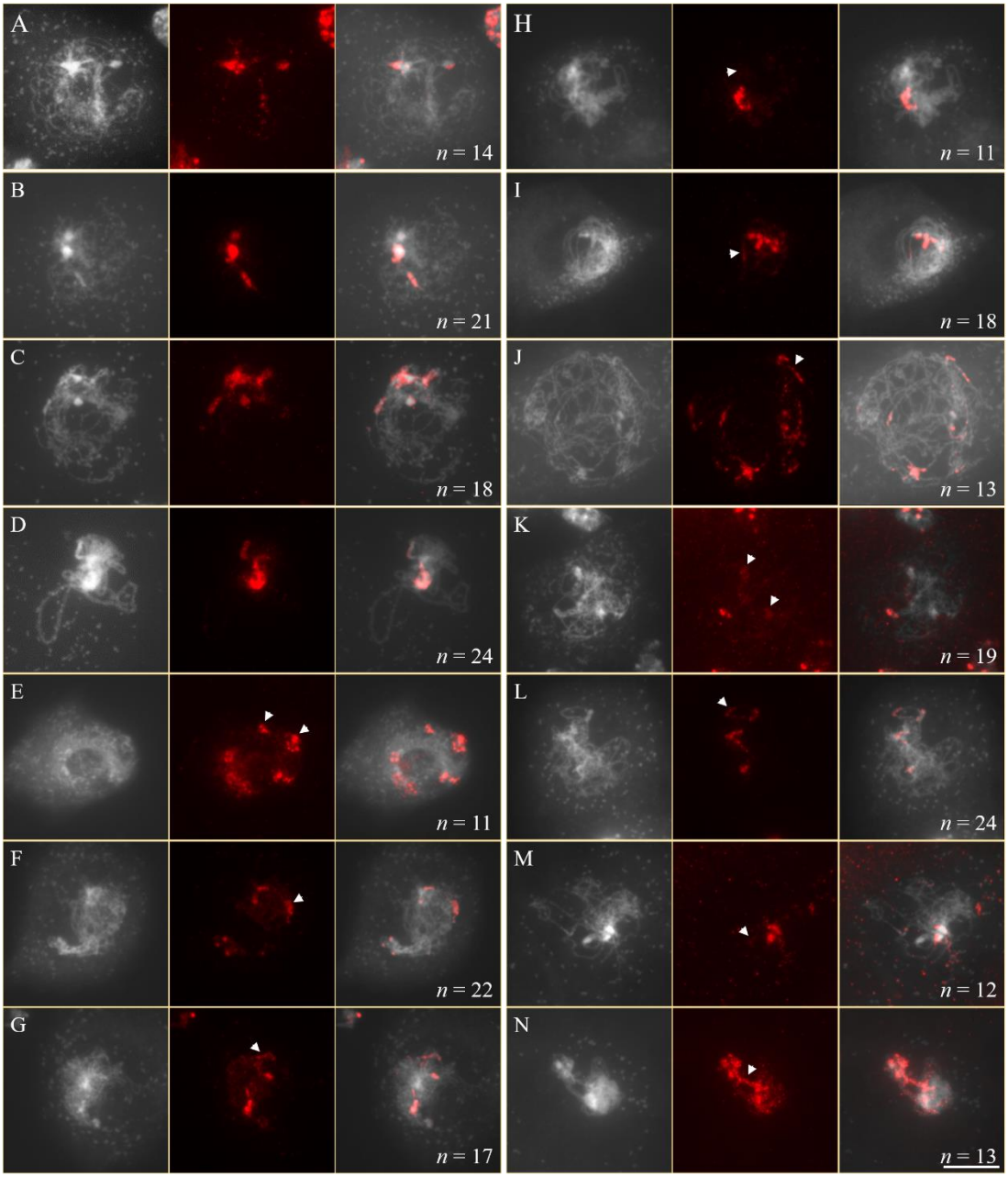

Figure 9. Immunolocalization of 5mC foci in wild-type Col-0 plants incubated at 20°C, 32°C and 36-38°C conditions. A-D, Leptotene (A), zygotene (B and C) and pachytene (D) chromosomes in Col-0 plants incubated at 20°C. E-I, Leptotene (E), zygotene (F and G) and pachytene (H and I) chromosomes in Col-0 plants incubated at 32°C. J-N, Leptotene (J), zygotene (K and L) and pachytene (M and N) chromosomes in Col-0 plants incubated at 36-38°C. The white arrows indicate regions with altered signals of 5mC. White: DAPI-stained chromosomes; Red: 5mC. *n* indicates the number of cells observed. Scale bar = 10 μm.

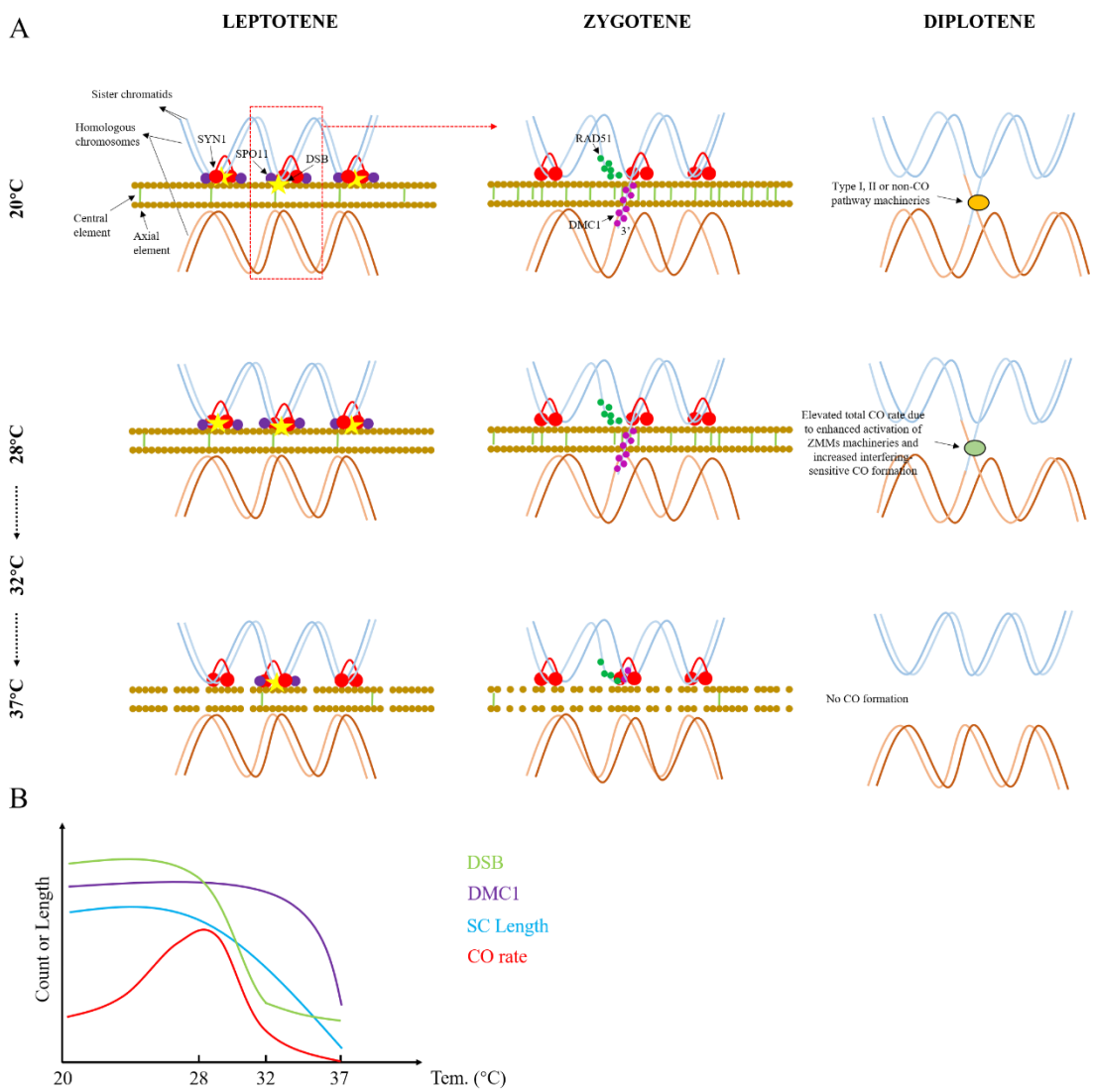

Figure 10. Proposed model explaining how increase of temperature modulates male MR in Arabidopsis. A, Behaviors of machineries involved in DSB formation, DSB repair and CO formation in Arabidopsis under elevated temperature conditions. B, Proposed correlation of the numbers of DSB and DMC1, SC length and CO rate in Arabidopsis to temperature increase.

Parsed Citations

Armstrong, S.J., Caryl, A.P., Jones, G.H., and Franklin, F.C. (2002). Asy1, a protein required for meiotic chromosome synapsis, localizes to axis-associated chromatin in Arabidopsis and Brassica. J Cell Sci 115, 3645-3655.
Google Scholar: Author Only Title Only Author and Title

Bai, X., Peirson, B.N., Dong, F., Xue, C., and Makaroff, C.A. (1999). Isolation and Characterization of SYN1, a RAD21-like Gene Essential for Meiosis in Arabidopsis. Plant Cell 11, 417-430.
Google Scholar: Author Only Title Only Author and Title

Barakate, A., Higgins, J.D., Vivera, S., Stephens, J., Perry, R.M., Ramsay, L., Colas, I., Oakey, H., Waugh, R., Franklin, F.C., Armstrong, S.J., and Halpin, C. (2014). The synaptonemal complex protein ZYP1 is required for imposition of meiotic crossovers in barley. Plant Cell 26, 729-740.
Google Scholar: Author Only Title Only Author and Title

Bergerat, A., de Massy, B., Gadelle, D., Varoutas, P.-C., Nicolas, A., and Forterre, P. (1997). An atypical topoisomerase II from archaea with implications for meiotic recombination. Nature 386, 414-417.
Google Scholar: Author Only Title Only Author and Title

Bomblies, K., Higgins, J.D., and Yant, L. (2015). Meiosis evolves: adaptation to external and internal environments. New Phytol 208, 306-323.
Google Scholar: Author Only Title Only Author and Title

Börner, G.V., Kleckner, N., and Hunter, N. (2004). Crossover/noncrossover differentiation, synaptonemal complex formation, and regulatory surveillance at the leptotene/zygotene transition of meiosis. Cell 117, 29-45.
Google Scholar: Author Only Title Only Author and Title

Brown, S.D., Mpaulo, S.J., Asogwa, M.N., Jézéquel, M., Whitby, M.C., and Lorenz, A. (2019). DNA sequence differences are determinants of meiotic recombination outcome. Sci Rep 9, 16446.
Google Scholar: Author Only Title Only Author and Title

Carballo, J.A., Johnson, A.L., Sedgwick, S.G., and Cha, R.S. (2008). Phosphorylation of the axial element protein Hop1 by Mec1/Tel1 ensures meiotic interhomolog recombination. Cell 132, 758-770.
Google Scholar: Author Only Title Only Author and Title

Chambon, A., West, A., Vezon, D., Horlow, C., De Muyt, A., Chelysheva, L., Ronceret, A., Darbyshire, A., Osman, K., Heckmann, S., Franklin, F.C.H., and Grelon, M. (2018). Identification of ASYNAPTIC4, a component of the meiotic chromosome axis. Plant Physiol 178, 233-246.
Google Scholar: Author Only Title Only Author and Title

Chang, Y.-N., Zhu, C., Jiang, J., Zhang, H., Zhu, J.-K., and Duan, C.-G. (2020). Epigenetic regulation in plant abiotic stress responses. Journal of Integrative Plant Biology 62, 563-580.
Google Scholar: Author Only Title Only Author and Title

Chelysheva, L., Grandont, L., Vrielynck, N., Guin, S.I., Mercier, R., and Grelon, M. (2010). An easy protocol for studying chromatin and recombination protein dynamics during Arabidopsis thaliana meiosis: immunodetection of cohesins, histones and MLH1. Cytogenetic and Genome Research 129, 143-153.
Google Scholar: Author Only Title Only Author and Title

Choi, K., Zhao, X., Kelly, K.A., Venn, O., Higgins, J.D., Yelina, N.E., Hardcastle, T.J., Ziolkowski, P.A., Copenhaver, G.P., Franklin, F.C., McVean, G., and Henderson, I.R. (2013). Arabidopsis meiotic crossover hot spots overlap with H2A.Z nucleosomes at gene promoters. Nature Genetics 45, 1327-1336.
Google Scholar: Author Only Title Only Author and Title

Choi, K., Zhao, X., Tock, A.J., Lambing, C., Underwood, C.J., Hardcastle, T.J., Serra, H., Kim, J., Cho, H.S., Kim, J., Ziolkowski, P.A., Yelina, N.E., Hwang, I., Martienssen, R.A., and Henderson, I.R. (2018). Nucleosomes and DNA methylation shape meiotic DSB frequency in Arabidopsis thaliana transposons and gene regulatory regions. Genome Res 28, 532-546.
Google Scholar: Author Only Title Only Author and Title

Cloud, V., Chan, Y.L., Grubb, J., Budke, B., and Bishop, D.K. (2012). Rad51 is an accessory factor for Dmc1-mediated joint molecule formation during meiosis. Science 337, 1222-1225.
Google Scholar: Author Only Title Only Author and Title

Coulton, A., Burridge, A.J., and Edwards, K.J. (2020). Examining the effects of temperature on recombination in Wheat. Frontiers in Plant Science 11.
Google Scholar: Author Only Title Only Author and Title

Da Ines, O., Degroote, F., Goubely, C., Amiard, S., Gallego, M.E., and White, C.I. (2013). Meiotic recombination in Arabidopsis is catalysed by DMC1, with RAD51 playing a supporting role. Plos Genetics 9, e1003787.
Google Scholar: Author Only Title Only Author and Title

De Muyt, A., Vezon, D., Gendrot, G., Gallois, J.-L., Stevens, R., and Grelon, M. (2007). AtPRD1 is required for meiotic double strand

break formation in Arabidopsis thaliana. EMBO Journal 26, 4126-4137.
Google Scholar: Author Only Title Only Author and Title

De Storme, N., and Geelen, D. (2020). High temperatures alter cross-over distribution and induce male meiotic restitution in Arabidopsis thaliana. Communications Biology 3, 187.
Google Scholar: Author Only Title Only Author and Title

De Storme, N., Copenhaver, G.P., and Geelen, D. (2012). Production of diploid male gametes in Arabidopsis by cold-induced destabilization of postmeiotic radial microtubule arrays. Plant Physiology 160, 1808-1826.
Google Scholar: Author Only Title Only Author and Title

Draeger, T., A, C.M., Alabdullah, A.K., Pendle, A., Rey, M.D., Shaw, P., and Moore, G. (2019). Dmc1 is a candidate for temperature tolerance during wheat meiosis. Theor Appl Genet.
Google Scholar: Author Only Title Only Author and Title

Ferdous, M., Higgins, J.D., Osman, K., Lambing, C., Roitinger, E., Mechtler, K., Armstrong, S.J., Perry, R., Pradillo, M., Cuñado, N., and Franklin, F.C.H. (2012). Inter-homolog crossing-over and synapsis in Arabidopsis meiosis are dependent on the chromosome axis protein AtASY3. Plos Genetics 8, e1002507-e1002507.
Google Scholar: Author Only Title Only Author and Title

Francis, K.E., Lam, S.Y., Harrison, B.D., Bey, A.L., Berchowitz, L.E., and Copenhaver, G.P. (2007). Pollen tetrad-based visual assay for meiotic recombination in Arabidopsis. The Proceedings of the National Academy of Sciences 104, 3913-3918.
Google Scholar: Author Only Title Only Author and Title

Grelon, M., Vezon, D., Gendrot, G., and Pelletier, G. (2001). AtSPO11-1 is necessary for efficient meiotic recombination in plants. Embo j 20, 589-600.
Google Scholar: Author Only Title Only Author and Title

Hartung, F., and Puchta, H. (2000). Molecular characterisation of two paralogous SPO11 homologues in Arabidopsis thaliana. Nucleic acids research 28, 1548-1554.
Google Scholar: Author Only Title Only Author and Title

Hartung, F., and Puchta, H. (2001). Molecular characterization of homologues of both subunits A (SPO11) and B of the archaebacterial topoisomerase 6 in plants. Gene 271, 81-86.
Google Scholar: Author Only Title Only Author and Title

Hartung, F., Wurz-Wildersinn, R., Fuchs, J., Schubert, I., Suer, S., and Puchta, H. (2007). The catalytically active tyrosine residues of both SPO11-1 and SPO11-2 are required for meiotic double-strand break induction in Arabidopsis. Plant Cell 19, 3090-3099.
Google Scholar: Author Only Title Only Author and Title

He, Y., Wang, M., Dukowic-Schulze, S., Zhou, A., Tiang, C.L., Shilo, S., Sidhu, G.K., Eichten, S., Bradbury, P., Springer, N.M., Buckler, E.S., Levy, A.A., Sun, Q., Pillardy, J., Kianian, P.M.A., Kianian, S.F., Chen, C., and Pawlowski, W.P. (2017). Genomic features shaping the landscape of meiotic double-strand-break hotspots in maize. Proc Natl Acad Sci U S A 114, 12231-12236.
Google Scholar: Author Only Title Only Author and Title

Higgins, J.D., Sanchez-Moran, E., Armstrong, S.J., Jones, G.H., and Franklin, F.C. (2005). The Arabidopsis synaptonemal complex protein ZYP1 is required for chromosome synapsis and normal fidelity of crossing over. Genes Dev 19, 2488-2500.
Google Scholar: Author Only Title Only Author and Title

Higgins, J.D., Perry, R.M., Barakate, A., Ramsay, L., Waugh, R., Halpin, C., Armstrong, S.J., and Franklin, F.C.H. (2012). Spatiotemporal asymmetry of the meiotic program underlies the predominantly distal distribution of meiotic crossovers in barley. The Plant cell 24, 4096-4109.
Google Scholar: Author Only Title Only Author and Title

Hotta, Y., Fujisawa, M., Tabata, S., Stern, H., and Yoshida, S. (1988). The effect of temperature on recombination activity in testes of rodents. Exp Cell Res 178, 163-168.
Google Scholar: Author Only Title Only Author and Title

Huang, J., Wang, C., Wang, H., Lu, P., Zheng, B., Ma, H., Copenhaver, G.P., and Wang, Y. (2019). Meiocyte-specific and AtSPO11-1–dependent small RNAs and their association with meiotic gene expression and recombination. Plant Cell 31, 444-464.
Google Scholar: Author Only Title Only Author and Title

Kim, J., and Choi, K. (2019). Signaling-mediated meiotic recombination in plants. Current Opinion in Plant Biology 51, 44-50.
Google Scholar: Author Only Title Only Author and Title

Kurzbauer, M.T., Uanschou, C., Chen, D., and Schlogelhofer, P. (2012). The recombinases DMC1 and RAD51 are functionally and spatially separated during meiosis in Arabidopsis. Plant Cell 24, 2058-2070.
Google Scholar: Author Only Title Only Author and Title

Lambing, C., Franklin, F.C., and Wang, C.R. (2017). Understanding and manipulating meiotic recombination in plants. Plant Physiol 173, 1530-1542.
Google Scholar: Author Only Title Only Author and Title

Lambing, C., Kuo, P.C., Tock, A.J., Topp, S.D., and Henderson, I.R. (2020a). ASY1 acts as a dosage-dependent antagonist of telomere-

led recombination and mediates crossover interference in Arabidopsis. Proc Natl Acad Sci U S A 117, 13647-13658.
Google Scholar: Author Only Title Only Author and Title

Lambing, C., Tock, A.J., Topp, S.D., Choi, K., Kuo, P.C., Zhao, X., Osman, K., Higgins, J.D., Franklin, F.C.H., and Henderson, I.R. (2020b). Interacting genomic landscapes of REC8-cohesin, chromatin, and meiotic recombination in Arabidopsis. Plant Cell 32, 1218-1239.
Google Scholar: Author Only Title Only Author and Title

Lambing, C., Osman, K., Nuntasoontorn, K., West, A., Higgins, J.D., Copenhaver, G.P., Yang, J., Armstrong, S.J., Mechtler, K., Roitinger, E., and Franklin, F.C. (2015). Arabidopsis PCH2 mediates meiotic chromosome remodeling and maturation of crossovers. Plos Genetics 11, e1005372.
Google Scholar: Author Only Title Only Author and Title

Lan, W.-H., Lin, S.-Y., Kao, C.-Y., Chang, W.-H., Yeh, H.-Y., Chang, H.-Y., Chi, P., and Li, H.-W. (2020). Rad51 facilitates filament assembly of meiosis-specific Dmc1 recombinase. Proc Natl Acad Sci U S A 117, 11257-11264.
Google Scholar: Author Only Title Only Author and Title

Lei, X., Ning, Y., Eid Elesawi, I., Yang, K., Chen, C., Wang, C., and Liu, B. (2020). Heat stress interferes with chromosome segregation and cytokinesis during male meiosis in Arabidopsis thaliana. Plant Signaling & Behavior 15, 1746985.
Google Scholar: Author Only Title Only Author and Title

Liao, Y., Smyth, G.K., and Shi, W. (2014). featureCounts: an efficient general purpose program for assigning sequence reads to genomic features. Bioinformatics 30, 923-930.
Google Scholar: Author Only Title Only Author and Title

Liu, B., De Storme, N., and Geelen, D. (2018). Cold-induced male meiotic restitution in Arabidopsis thaliana is not mediated by GA-DELLA signaling. Frontiers in Plant Science 9, 91.
Google Scholar: Author Only Title Only Author and Title

Liu, B., Mo, W.J., Zhang, D., De Storme, N., and Geelen, D. (2019). Cold influences male reproductive development in plants: a hazard to fertility, but a window for evolution. Plant Cell Physiology 60, 7-18.
Google Scholar: Author Only Title Only Author and Title

Lloyd, A., Morgan, C., H. Franklin, F.C., and Bomblies, K. (2018). Plasticity of Meiotic Recombination Rates in Response to Temperature in Arabidopsis. Genetics 208, 1409-1420.
Google Scholar: Author Only Title Only Author and Title

Mai, Y., Li, H., Suo, Y., Fu, J., Sun, P., Han, W., Diao, S., and Li, F. (2019). High temperature treatment generates unreduced pollen in persimmon (Diospyros kaki Thunb.). Scientia Horticulturae 258, 108774.
Google Scholar: Author Only Title Only Author and Title

Milman, N., Higuchi, E., and Smith, G.R. (2009). Meiotic DNA double-strand break repair requires two nucleases, MRN and Ctp1, to produce a single size class of Rec12 (Spo11)-oligonucleotide complexes. Molecular and cellular biology 29, 5998-6005.
Google Scholar: Author Only Title Only Author and Title

Modliszewski, J.L., and Copenhaver, G.P. (2017). Meiotic recombination gets stressed out: CO frequency is plastic under pressure. Current Opinion in Plant Biology 36, 95-102.
Google Scholar: Author Only Title Only Author and Title

Modliszewski, J.L., Wang, H., Albright, A.R., Lewis, S.M., Bennett, A.R., Huang, J., Ma, H., Wang, Y., and Copenhaver, G.P. (2018). Elevated temperature increases meiotic crossover frequency via the interfering (Type I) pathway in Arabidopsis thaliana. Plos Genetics 14, e1007384.
Google Scholar: Author Only Title Only Author and Title

Morgan, C.H., Zhang, H., and Bomblies, K. (2017). Are the effects of elevated temperature on meiotic recombination and thermotolerance linked via the axis and synaptonemal complex? Philos Trans R Soc Lond B Biol Sci 372, 20160470.
Google Scholar: Author Only Title Only Author and Title

Neale, M.J., Pan, J., and Keeney, S. (2005). Endonucleolytic processing of covalent protein-linked DNA double-strand breaks. Nature 436, 1053-1057.
Google Scholar: Author Only Title Only Author and Title

Nibau, C., Lloyd, A., Dadarou, D., Betekhtin, A., Tsilimigka, F., Phillips, D.W., and Doonan, J.H. (2020). CDKG1 is required for meiotic and somatic recombination intermediate processing in Arabidopsis. Plant Cell 32, 1308-1322.
Google Scholar: Author Only Title Only Author and Title

Oliver, C., Santos, J.L., and Pradillo, M. (2016). Accurate chromosome segregation at first meiotic division requires AGO4, a protein involved in RNA-dependent DNA methylation in Arabidopsis thaliana. Genetics 204, 543-553.
Google Scholar: Author Only Title Only Author and Title

Parra-Rojas, J.P., Largo-Gosens, A., Carrasco, T., Celiz-Balboa, J., Arenas-Morales, V., Sepúlveda-Orellana, P., Temple, H., Sanhueza, D., Reyes, F.C., Meneses, C., Saez-Aguayo, S., and Orellana, A. (2019). New steps in mucilage biosynthesis revealed by analysis of the transcriptome of the UDP-rhamnose/UDP-galactose transporter 2 mutant. Journal of Experimental Botany 70, 5071-5088.
Google Scholar: Author Only Title Only Author and Title

Pertea, M., Kim, D., Pertea, G.M., Leek, J.T., and Salzberg, S.L. (2016). Transcript-level expression analysis of RNA-seq experiments with HISAT, StringTie and Ballgown. Nat Protoc 11, 1650-1667.
Google Scholar: Author Only Title Only Author and Title

Pohl, T.J., and Nickoloff, J.A. (2008). Rad51-independent interchromosomal double-strand break repair by gene conversion requires Rad52 but not Rad55, Rad57, or Dmc1. Molecular and cellular biology 28, 897-906.
Google Scholar: Author Only Title Only Author and Title

Puizina, J., Siroky, J., Mokros, P., Schweizer, D., and Riha, K. (2004). Mre11 deficiency in Arabidopsis is associated with chromosomal instability in somatic cells and Spo11-dependent genome fragmentation during meiosis. The Plant cell 16, 1968-1978.
Google Scholar: Author Only Title Only Author and Title

Sanchez-Moran, E., Santos, J.L., Jones, G.H., and Franklin, F.C. (2007). ASY1 mediates AtDMC1-dependent interhomolog recombination during meiosis in Arabidopsis. Genes Dev 21, 2220-2233.
Google Scholar: Author Only Title Only Author and Title

Sanchez-Moran, E., Osman, K., Higgins, J.D., Pradillo, M., Cunado, N., Jones, G.H., and Franklin, F.C. (2008). ASY1 coordinates early events in the plant meiotic recombination pathway. Cytogenet Genome Res 120, 302-312.
Google Scholar: Author Only Title Only Author and Title

Singh, G., Da Ines, O., Gallego, M.E., and White, C.I. (2017). Analysis of the impact of the absence of RAD51 strand exchange activity in Arabidopsis meiosis. Plos One 12, e0183006.
Google Scholar: Author Only Title Only Author and Title

Smith, G.R., Boddy, M.N., Shanahan, P., and Russell, P. (2003). Fission yeast Mus81.Eme1 Holliday junction resolvase is required for meiotic crossing over but not for gene conversion. Genetics 165, 2289-2293.
Google Scholar: Author Only Title Only Author and Title

Stacey, N.J., Kuromori, T., Azumi, Y., Roberts, G., Breuer, C., Wada, T., Maxwell, A., Roberts, K., and Sugimoto-Shirasu, K. (2006). Arabidopsis SPO11-2 functions with SPO11-1 in meiotic recombination. Plant J 48, 206-216.
Google Scholar: Author Only Title Only Author and Title

Su, H., Cheng, Z., Huang, J., Lin, J., Copenhaver, G.P., Ma, H., and Wang, Y. (2017). Arabidopsis RAD51, RAD51C and XRCC3 proteins form a complex and facilitate RAD51 localization on chromosomes for meiotic recombination. Plos Genetics 13, e1006827.
Google Scholar: Author Only Title Only Author and Title

Sugimoto-Shirasu, K., Stacey, N.J., Corsar, J., Roberts, K., and McCann, M.C. (2002). DNA topoisomerase VI is essential for endoreduplication in Arabidopsis. Curr Biol 12, 1782-1786.
Google Scholar: Author Only Title Only Author and Title

Uanschou, C., Siwiec, T., Pedrosa-Harand, A., Kerzendorfer, C., Sanchez-Moran, E., Novatchkova, M., Akimcheva, S., Woglar, A., Klein, F., and Schlögelhofer, P. (2007). A novel plant gene essential for meiosis is related to the human CtIP and the yeast COM1/SAE2 gene. Embo j 26, 5061-5070.
Google Scholar: Author Only Title Only Author and Title

Uanschou, C., Ronceret, A., Von Harder, M., De Muyt, A., Vezon, D., Pereira, L., Chelysheva, L., Kobayashi, W., Kurumizaka, H., Schlögelhofer, P., and Grelon, M. (2013). Sufficient amounts of functional HOP2/MND1 complex promote interhomolog DNA repair but are dispensable for intersister DNA repair during meiosis in Arabidopsis. Plant Cell 25, 4924-4940.
Google Scholar: Author Only Title Only Author and Title

Underwood, C.J., Choi, K., Lambing, C., Zhao, X., Serra, H., Borges, F., Simorowski, J., Ernst, E., Jacob, Y., Henderson, I.R., and Martienssen, R.A. (2018). Epigenetic activation of meiotic recombination near Arabidopsis thaliana centromeres via loss of H3K9me2 and non-CG DNA methylation. Genome Res 28, 519-531.
Google Scholar: Author Only Title Only Author and Title

Vignard, J., Siwiec, T., Chelysheva, L., Vrielynck, N., Gonord, F., Armstrong, S.J., Schlögelhofer, P., and Mercier, R. (2007). The interplay of RecA-related proteins and the MND1-HOP2 complex during meiosis in Arabidopsis thaliana. Plos Genetics 3, 1894-1906.
Google Scholar: Author Only Title Only Author and Title

Wang, H., Xu, W., Sun, Y., Lian, Q., Wang, C., Yu, C., He, C., Wang, J., Ma, H., Copenhaver, G.P., and Wang, Y. (2020). The cohesin loader SCC2 contains a PHD finger that is required for meiosis in land plants. Plos Genetics 16, e1008849.
Google Scholar: Author Only Title Only Author and Title

Wang, J., Li, D., Shang, F., and Kang, X. (2017). High temperature-induced production of unreduced pollen and its cytological effects in Populus. Scientific Reports 7, 5281.
Google Scholar: Author Only Title Only Author and Title

Wang, Y., and Copenhaver, G.P. (2018). Meiotic recombination: mixing it up in plants. Annual Review of Plant Biology 69, 577-609.
Google Scholar: Author Only Title Only Author and Title

Wang, Y., Cheng, Z., Lu, P., Timofejeva, L., and Ma, H. (2014). Molecular cell biology of male meiotic chromosomes and isolation of male meiocytes in Arabidopsis thaliana. Methods Mol Biol 1110, 217-230.
Google Scholar: Author Only Title Only Author and Title

Xue, M., Wang, J., Jiang, L., Wang, M., Wolfe, S., Pawlowski, W.P., Wang, Y., and He, Y. (2018). The number of meiotic double-strand breaks influences crossover distribution in Arabidopsis. Plant Cell 30, 2628-2638.
Google Scholar: Author Only Title Only Author and Title

Yamada, S., Kugou, K., Ding, D.-Q., Fujita, Y., Hiraoka, Y., Murakami, H., Ohta, K., and Yamada, T. (2017). The histone variant H2A.Z promotes initiation of meiotic recombination in fission yeast. Nucleic acids research 46, 609-620.
Google Scholar: Author Only Title Only Author and Title

Yang, C., Sofroni, K., Wijnker, E., Hamamura, Y., Carstens, L., Harashima, H., Stolze, S.C., Vezon, D., Chelysheva, L., Orban-Nemeth, Z., Pochon, G., Nakagami, H., Schlogelhofer, P., Grelon, M., and Schnittger, A. (2019). The Arabidopsis Cdk1/Cdk2 homolog CDKA;1 controls chromosome axis assembly during plant meiosis. Embo j, e101625.
Google Scholar: Author Only Title Only Author and Title

Yelina, N.E., Lambing, C., Hardcastle, T.J., Zhao, X., Santos, B., and Henderson, I.R. (2015). DNA methylation epigenetically silences crossover hot spots and controls chromosomal domains of meiotic recombination in Arabidopsis. Genes Dev 29, 2183-2202.
Google Scholar: Author Only Title Only Author and Title

Yoshida, T., Ohama, N., Nakajima, J., Kidokoro, S., Mizoi, J., Nakashima, K., Maruyama, K., Kim, J.M., Seki, M., Todaka, D., Osakabe, Y., Sakuma, Y., Schöffl, F., Shinozaki, K., and Yamaguchi-Shinozaki, K. (2011). Arabidopsis HsfA1 transcription factors function as the main positive regulators in heat shock-responsive gene expression. Mol Genet Genomics 286, 321-332.
Google Scholar: Author Only Title Only Author and Title

Yu, S., Galvão, V.C., Zhang, Y.-C., Horrer, D., Zhang, T.-Q., Hao, Y.-H., Feng, Y.-Q., Wang, S., Schmid, M., and Wang, J.-W. (2012). Gibberellin regulates the Arabidopsis floral transition through miR156-targeted SQUAMOSA PROMOTER BINDING–LIKE transcription factors. Plant Cell 24, 3320-3332.
Google Scholar: Author Only Title Only Author and Title

Zhang, K., Wu, X.C., Zheng, D.Q., and Petes, T.D. (2017). Effects of temperature on the meiotic recombination landscape of the yeast Saccharomyces cerevisiae. mBio 8.
Google Scholar: Author Only Title Only Author and Title

Zhang, X., Yazaki, J., Sundaresan, A., Cokus, S., Chan, S.W.L., Chen, H., Henderson, I.R., Shinn, P., Pellegrini, M., Jacobsen, S.E., and Ecker, Joseph R. (2006). Genome-wide high-resolution mapping and functional analysis of DNA methylation in Arabidopsis. Cell 126, 1189-1201.
Google Scholar: Author Only Title Only Author and Title

Zheng, T., Nibau, C., Phillips, D.W., Jenkins, G., Armstrong, S.J., and Doonan, J.H. (2014). CDKG1 protein kinase is essential for synapsis and male meiosis at high ambient temperature in Arabidopsis thaliana. Proceedings of the National Academy of Sciences of the United States of America 111, 2182-2187.
Google Scholar: Author Only Title Only Author and Title

Zickler, D., and Kleckner, N. (1999). Meiotic chromosomes: integrating structure and function. Annu Rev Genet 33, 603-754.
Google Scholar: Author Only Title Only Author and Title